# Cache Creek Settling Basin / Yolo Bypass Project
# Contract No. 4600010003

# Cache Creek Settling Basin Trap Efficiency Study
# Progress Report
# April 15, 2013 – April 30, 2014

Prepared for

## California Department of Water Resources

Prepared By

Kara Carr
Ali Ercan
Tongbi Tu
Hossein Bandeh
M. Levent Kavvas (Principal Investigator)

## UC Davis J. A. Hydraulics Laboratory

Department of Civil and Environmental Engineering
University of California, Davis
One Shields Avenue
Davis, CA 95616

**May 1, 2014**
**Revised September 23, 2015**

Table of Contents

List of Figures ..... 2
List of Tables ..... 5
Acknowledgements ..... 6
1 Introduction ..... 6
1.1 Background ..... 7
1.2 Objective ..... 8
2 Flow Sampling by UCDJAHL ..... 9
3 Two-dimensional Flow and Sediment Transport Model ..... 9
3.1 CCHE2D ..... 10
3.2 Third-party Calibration and Validation ..... 10
3.2.1 NCCHE Calibration and Validation ..... 11
3.2.2 Non-Principal Calibration and Validation ..... 17
4 CCHE2D Flow Simulations ..... 22
4.1.1 Calibration by 18-22 March 2011 event at Road 102 ..... 29
4.1.2 Validation by 18-22 March 2011 flow event inside CCSB ..... 32
4.1.3 Validation by 23-27 March 2011 flow event at Road 102 and inside CCSB ..... 47
5 References ..... 67
Appendix ..... 69

**LIST OF FIGURES**

Figure 3.1. Flume dimension and recirculation pattern of Xie (1994) experiments (from Jia and Wang, 2001b) ..... 11
Figure 3.2 Comparisons of the simulated (line) and measured (circles) flow field in the channel of sudden expansion, a: Q=0.01815m$^3$/s, b: Q=0.03854m$^3$/s (Jia and Wang, 2001b) ..... 12
Figure 3.3 Mesh system of the 180-degree U-shaped channel (Jia and Wang, 2001b) ..... 13
Figure 3.4 Simulated and measured velocities of the 180-degree U-shaped channel (Jia and Wang, 2001b) ..... 13
Figure 3.5 Definition sketch of the compound channel components (Jia and Wang, 2001b) ..... 14
Figure 3.6 Comparison of measured and simulated velocity in a compound channel (Jia and Wang, 2001b) ..... 14
Figure 3.7 Comparison of measured and simulated bed elevations, bed aggradation experiment (Jia and Wang, 2001b) ..... 15
Figure 3.8 Comparison of experimental and simulated results, bed degradation experiment (Jia and Wang, 2001b) ..... 16
Figure 3.9. Suspended sediment verification results, River Nechar, Germany: a. sediment concentration contour plot; b. comparison of measured and computed sediment concentrations (Jia and Wang, 2001b) ..... 17
Figure 3.10 Flow field from (a) UVP (b) LSPIV (c) CCHE2D and (d) comparison of velocity magnitude vectors obtained from all three methods ..... 18
Figure 3.11 Experimental set-up for meandering compound channel Mohanty et al. (2012) ..... 19
Figure 3.12 Normalized depth averaged velocity diagrams for each of the five runs (a) Run 1 (b) Run 2 (c) Run 3 (d) Run 4 (e) Run 5 (Mohanty et al., 2012) .. 19
Figure 3.13 Shear velocity diagrams for each of the five runs (a) Run 1 (b) Run 2 (c) Run 3 (d) Run 4 (e) Run 5, (Mohanty et al., 2012) ..... 20
Figure 3.14 Huang (2000) Channel degradation comparison, utilizing each bed roughness method for (a) Wu et al. (2000) bed-load formula, (b) Wu et al. (2000) bed-material load formula, (c) Modified Ackers–White bed-material formula, (d) Modified Engelund–Hansen bed-material load formula and (e) SEDTRA module ..... 21
Figure 3.15 Calibration results for cross section bed level in 2003 (a) section 13 and (b) section 16 (Negm et al., 2010) ..... 22
Figure 3.16 Verification results for cross section bed level in 2007 (a) section 13 and (b) section 16 (Negm et al., 2010) ..... 22
Figure 3.17 Predicted bed elevation for sections 13 and 16 plotted against corresponding measured bed elevation (Negm et al., 2010) ..... 22
Figure 4.1 Mesh from Cache Creek at Yolo to Road 102 ..... 24
Figure 4.2 Simulation Mesh for CCSB ..... 25
Figure 4.3 Elevation contour of simulated extent from Cache Creek at Yolo to Rd 102 ..... 26
Figure 4.4 Elevation contour of simulated extent, Rd 102 through CCSB including approximate locations of result comparison points ..... 27

Figure 4.5 Rating curve for the USGS site 11452800, CCSB overflow weir. .....28
Figure 4.6 Rating curve for USGS site 11452900, CCSB low flow culvert. .....28
Figure 4.7 (a) Results of CCHE2D water surface elevation at Rd 102 for various bed roughness and measured water surface elevation at Rd 102, and (b) percent error of simulated water surface elevations for various bed roughness methods31
Figure 4.8 (a) Results of CCHE2D water surface elevation at Rd 102 for various grain size distributions, (b) percent error of simulated water surface elevations at Rd 102 for various grain size distributions .....32
Figure 4.9 Comparison plots of 18-22 March 2011 simulation, (a) Inflow discharge at Cache Creek at Yolo with time steps for results display, (b) Calibrated water surface elevation at Rd 102 for entire simulation duration, (c) Water Surface Elevation validation at Site C for entire simulation duration, (d) Water Surface Elevation validation at Overflow Weir for entire simulation duration .....34
Figure 4.10 Water depth results at selected times on rising limb of storm hydrograph, 1 and 2 (peak flow) of 18-22 March 2011 event; Cache Creek at Yolo to Rd 102 .....35
Figure 4.11 Water depth results at selected times on falling limb of hydrograph, 3 and 4 of 18-22 March 2011 event; Cache Creek at Yolo to Rd 102.....36
Figure 4.12 Velocity magnitude results at selected times on rising limb of hydrograph, 1 and 2 (peak flow) of 18-22 March 2011 event; Cache Creek at Yolo to Rd 102 .....37
Figure 4.13 Velocity magnitude results at selected times on falling limb of hydrograph, 3 and 4 of 18-22 March 2011 event; Cache Creek at Yolo to Rd 102 .....38
Figure 4.14 CCSB water depth results, March 2011, at selected times on rising limb of hydrograph, 1 and 2 (peak flow) of 18-22 March 2011 event. .....39
Figure 4.15 CCSB water depth results, March 2011, at selected times on falling limb of hydrograph, 3 and 4 of 18-22 March 2011 event.....40
Figure 4.16 CCSB velocity magnitude results, March 2011, at selected times on rising limb of hydrograph, 1 and 2 (peak flow) of 18-22 March 2011 event.....41
Figure 4.17 CCSB velocity magnitude results, March 2011, at selected times on falling limb of hydrograph, 3 and 4 of 18-22 March 2011 event .....42
Figure 4.18 CCSB velocity magnitude result with scaled directional vectors, at selected time 1 of 18-22 March 2011 event .....43
Figure 4.19 CCSB velocity magnitude result with scaled directional vectors, at selected time 2 of 18-22 March 2011 event .....44
Figure 4.20 CCSB velocity magnitude result with scaled directional vectors, at selected time 3 of 18-22 March 2011 event .....45
Figure 4.21 CCSB velocity magnitude result with scaled directional vectors, at selected time 4 of 18-22 March 2011 event .....46
Figure 4.22 Comparison plots of 23-27 March 2011 validation simulation, (a) Inflow discharge at Cache Creek at Yolo with time steps for results display, (b) Water surface elevation validation at Rd 102 for entire simulation duration, (c) Water Surface Elevation validation at Site C for entire simulation duration, (d)

Water Surface Elevation validation at Overflow Weir for entire simulation duration .....48
Figure 4.23 Water depth validation simulation results, Yolo to Rd 102, at selected times 1 and 2 of 23-27 March 2011 event.....49
Figure 4.24 Water depth validation simulation results, Yolo to Rd 102, at selected times 3 (peak flow) and 4 of 23-27 March 2011 event .....50
Figure 4.25 Water depth validation simulation results, Yolo to Rd 102, at selected time 5 of 23-27 March 2011 event .....51
Figure 4.26 Water depth validation results, CCSB, at selected times 1 and 2 of 23-27 March 2011 event .....52
Figure 4.27 Water depth validation results, CCSB, at selected times 3 (peak flow) and 4 of 23-27 March 2011 event .....53
Figure 4.28 Water depth validation results, CCSB, at selected time 5 of 23-27 March 2011 event .....54
Figure 4.29 Velocity magnitude validation results, Yolo to Rd 102, at selected times 1 and 2 of 23-27 March 2011 event.....55
Figure 4.30 Velocity magnitude validation results, Yolo to Rd 102, at selected times 3 (peak flow) and 4 of 23-27 March 2011 event .....56
Figure 4.31 Velocity magnitude validation results, Yolo to Rd 102, at selected time 5 of 23-27 March 2011 event. .....57
Figure 4.32 Velocity magnitude validation simulation results, CCSB, at selected times 1 and 2 of 23-27 March 2011 event.....58
Figure 4.33 Velocity magnitude validation simulation results, CCSB, at selected times 3 (peak flow) and 4 of 23-27 March 2011 event .....59
Figure 4.34 Velocity magnitude validation simulation results, CCSB, at selected time 5 of 23-27 March 2011 event .....60
Figure 4.35 CCSB validation velocity magnitude result with scaled directional vectors, at selected time 1 of 23-27 March 2011 event.....62
Figure 4.36 CCSB validation velocity magnitude result with scaled directional vectors, at selected time 2 of 23-27 March 2011 event.....63
Figure 4.37 CCSB validation velocity magnitude result with scaled directional vectors, at selected time 3 (peak flow) of 23-27 March 2011 event .....64
Figure 4.38 CCSB validation velocity magnitude result with scaled directional vectors, at selected time 4 of 23-27 March 2011 event.....65
Figure 4.39 CCSB validation velocity magnitude result with scaled directional vectors, at selected time 5 of 23-27 March 2011 event.....66
Figure A.0.1 Dr. Ercan and Dr. Carr on the Sacramento River, ADCP Trial Run December 13, 2013 .....69
Figure A.0.2 Tracker Guide V-14 Boat purchased for sediment and velocity measurements within the CCSB .....69
Figure A.0.3 ADCP transmitter and float.....70

**LIST OF TABLES**

Table 3.1 Flow conditions for the sudden expansion channel experiments conducted by Xie (1994) and simulated by Jia and Wang, (2001b). ..... 11
Table 3.2 Flow conditions for the 180-degree U-shaped channel, (from Jia and Wang, 2001b). ..... 12
Table 3.3 Parameters of the compound channel experiment (Jia and Wang, 2001b). ..... 14
Table 3.4 Sediment and initial flow conditions, bed aggradation experiment performed by Soni (1981) (from Jia and Wang, 2001b). ..... 15
Table 3.5 Sediment and initial flow conditions, bed degradation experiment performed by Newton (1951) (from Jia and Wang, 2001b). ..... 16
Table 3.6 Hydraulic parameters for the experimental runs, meandering compound channel (Mohanty et al., 2006). ..... 19
Table 4.1 Grain size distributions applied with Wu and Wang (1999) roughness simulations. ..... 29
Table 4.2 Normalized root mean square error for simulated water surface elevations at Rd 102 for each bed roughness method. ..... 32
Table 4.3 NRMSE and Nash Coefficient for calibration and validation simulations. ..... 33

## ACKNOWLEDGEMENTS

We thank the personnel at U.S Geological Survey Sacramento Field Office for sharing sediment and flow data at Cache Creek Settling Basin.

This research was funded through a contract with the Department of Water Resources (Contract No. 4600010003). We thank Mr. Frederick Gius for his insight and support, and Mr. John Nosacka, who coordinated the efforts and resources between Department of Water Resources and UC Davis J. Amorocho Hydraulics Laboratory during the study,

## 1 INTRODUCTION

This report describes the Cache Creek Settling Basin (CCSB) / Yolo Bypass Project progress during April 15th, 2013 through April 14th, 2014. Objectives for this year of the study included:

Objective 1. A field measurement sampling program was to be conducted throughout the wet season to enable sampling of 2-D velocity and discharge along transects north of the low flow channel within the settling basin. Samples were to be taken at regular intervals during storm events and while sufficient water remains in the basin to facilitate sampling. These measurements were to be incorporated in 2-D flow and sediment transport models evaluation as they become available. This objective was not met as sufficient discharge did not occur in Year 1. There was no storm event during the study period which provided sufficient inundation of the CCSB. All supplies necessary for sampling were secured.

Objective 2. Field measurements as supplied by USGS were to be catalogued and incorporated into the 2-D flow and sediment transport models for updated calibration and validation as they become available. This objective was met, as all available data was catalogued and stored in our data bank. Additionally, field measurements were utilized in calibration and validation of the 2-dimensional flow and sediment transport model. Calibration and validation was possible for flows up to 15900 cubic feet per second (cfs), the largest discharge record supplied by USGS.

Year I Objective 3. 2-D flow and sediment transport model results were to be analyzed utilizing all the available flow and sediment data, and further data gaps noted. This objective was partially met. Hydrodynamic modeling has been validated for flows with an exceedance probability of 41-percent or more. Simulations of larger magnitude flows are not validated, and additional sampling of flow and sediment is required to increase confidence in the model's performance and applicability at larger discharge magnitudes. As previously identified, additional samples of coincident flow and sediment, taken periodically over the duration of a storm event, are required. Such samples were not

available in this year of the study due to lack of storm events within the study period. Further sediment grain size distribution and sediment concentration at the inlet and outlet of the CCSB are also necessary for validation of the sediment transport model.

### *1.1 Background*

Cache Creek Settling Basin, located two miles east of the City of Woodland, California, was originally built in 1938. The primary function of the CCSB is to remove a significant portion of the sediment load from Cache Creek to avoid its deposition in the Yolo Bypass, thereby preserving the capacity of the bypass for conveying flood flows. The Yolo Bypass serves to protect Sacramento and surrounding areas from flooding with a design flow of 216,000 cfs. Cache Creek delivers large amounts of sediment to the Settling Basin every year, and is the main source of mercury to the San Francisco Bay-Delta. In addition to preserving the flood flow capacity of the Yolo Bypass; entrapment of sediment in the Basin is instrumental in diminishing the mercury load to the San Francisco Bay-Delta, making the Basin fundamental in preserving water quality. The sediment entering the CCSB is a legacy of the California Gold Rush and mercury mining in California's Coastal range. A number of abandoned, un-reclaimed and partially reclaimed mercury mines are situated in the Cache Creek watershed. Furthermore, aggregate mining of Cache Creek has increased channel incision and sediment loading in the creek (Thayer, 2009).

The CCSB has been modified many times since 1938 in order to redistribute sediment settling patterns and increase sediment storage capacity. From 1991 to 1993, the Basin was radically altered. Surrounding levees were raised 12 feet, the training channel was relocated, and a new outlet weir was built 5 feet higher than the previous weir, representing the current conditions. At the time of alteration it was believed the Basin would retain 340 acre-feet of sediment per year, at a 55% trap efficiency, and that an additional 50 years of sediment storage was being provided. This postulated trap efficiency is based on an action plan outlined in the USACE 2007 Cache Creek Settling Basin Operations and Maintenance Manual, in which the outlet weir is to be raised an additional 6-feet at year 25 (2018) of the project, or when the trap-efficiency becomes 30%. Also beginning in year 25 of the project, 400-foot sections of the interior training levee will be removed every five years, starting with a section 1100 feet upstream from the current terminus of the training channel. Each subsequent 400-foot section will be removed 1100 feet upstream from the section that is removed previously.

In order to determine whether the trap-efficiency and sedimentation rate in the Basin are meeting design requirements set forth by USACE, the personnel at UC Davis J. Amorocho Hydraulics Laboratory (UCDJAHL) began evaluating the settling basin trap efficiency through application of the National Center for Computational Hydroscience and Engineering's CCHE2D model of two-dimensional depth averaged flow and sediment transport. The evaluation was

conducted with respect to the current Settling Basin design as defined by 2006 and 2008 surveys of the Basin, utilizing field measurements of suspended sediment and flow into, within, and out of the Cache Creek Settling Basin as provided by USGS, as well as by the physical sedimentation modeling performed at the UCDJAHL in 2009.

### *1.2 Objective*

The major objectives of this study are:

**i.** to perform field measurements by UCDJAHL staff of 2-D velocities and flow within the Settling Basin to be incorporated in calibration and validation of 2-D flow and sediment transport models. Because of the 2-D nature of flow in the basin and the desire to capture the 2-D spread of sediment within the basin, it is critical to capture internal transects, as well as inflow and outflow sections. Additionally, field measurements performed by UCDJAHL staff will provide a dense sampling of flow and velocity during storm events, capturing multiple samples as a storm hydrograph passes through the Basin.

**ii.** to incorporate flow and suspended sediment measurements provided by USGS in order to calibrate and validate the 2-D flow and sediment transport models. Currently available flow and sediment measurements are insufficient to support the simulations' claim of loading as they do not provide means of calculating loads into the basin, moving through the basin and exiting the basin. It is essential for calibration and validation of the models that these sediment measurements be concurrent with velocity/flow measurements. Additional data will ultimately result in a more reliable estimate of the settling basin trap efficiency with respect to current and future settling basin design.

Furthermore, UCDJAHL will provide DWR with a method of reevaluating sedimentation for any further augmentation proposals. Estimates of trap efficiency will be produced for a range of possible future climate conditions. The mean trap efficiency as well as the 95% confidence bands will be provided.

## 2 FLOW SAMPLING BY UCDJAHL

In order to calibrate and validate the 2-dimensional flow and sediment conditions within the CCSB, a flow measurement campaign has been initiated by the UCDJAHL. Dr. Ali Ercan and Dr. Kara Carr attended the formal USGS training course, “Streamflow Measurement using ADCP’s in November 2013. A StreamPro ADCP with all necessary components and software, boat and boating equipment, trailer, and suitable laptop were purchased throughout the final quarter of 2013. Trial measurements utilizing the equipment necessary in the CCSB sampling campaign were conducted in December 2013. See Attachment A for pictures.

When flow is present in the CCSB, north of the low flow channel, flow velocity will be sampled. Sampling transect locations will be determined by flow and inundation conditions. The StreamPro ADCP will be used for measurement of flow velocity. A GPS mounted on the ADCP unit will allow for recognition of sampling locations and application of collected data to calibration and validation of the two-dimensional flow and sediment discharge model.

Due to the lack of weather, flow and sediment measurements in the CCSB have not been collected by UCDJAHL at the time of this report.

## 3 TWO-DIMENSIONAL FLOW AND SEDIMENT TRANSPORT MODEL

Two-dimensional modeling was selected for representation of the CCSB, as vertical velocities and accelerations are believed to be small when compared with the significant 2-D horizontal velocities and accelerations. Selection of a suitable two-dimensional flow and sediment transport model was completed after identifying factors that are crucial to the success of the trap efficiency estimation.

These factors include:

1. accurate representation of the Basin's training channel which has changed significantly since its construction due to deposition of sediment;
2. routing of flow and sediment from the output of the Cache Creek watershed study (Cache Creek at Yolo) to the inlet of the CCSB at Road 102;
3. calibration and validation of the two-dimensional model with well-timed and well-placed measurements of flow and sediment properties;
4. long term simulations that encompass the full range of flows historically observed in the Basin as well as future predictions which incorporate climatic uncertainty;
5. simulations of flow which represent the transience of both sediment loads and flows entering the CCSB.

### *3.1 CCHE2D*

Developed at the National Center for Computation Hydroscience and Engineering at the University of Mississippi (NCCHE), CCHE2D is a two-dimensional depth averaged unsteady flow and sediment transport model. CCHE2D simulates the movement of water, and both cohesive and non-cohesive sediment. Flow modeling is based on depth-averaged Navier-Stokes equations, while sediment transport is modeled as total load by solving the depth-averaged convection-diffusion equation of the suspended sediment load, and the continuity equation of bed load. The system of equations is discretized using the Efficient Element Method, a finite element method described by Wang and Hu (1992). Detailed description of the solution method can be found in the CCHE2D Technical Manual (Jia and Wang, 2001a). The model provides user options in the sediment transport description. Five sediment transport formulas are available; Wu et al. (2000) bed-load formula, Wu et al. (2000) bed-material load formula, Modified Ackers–White bed-material formula (Proffit and Sutherland, 1983), Modified Engelund–Hansen bed-material load formula (Engelund and Hansen, 1967) and SEDTRA module (Garbrecht et al., 1995) for bed-material load. There are three methods for estimating Manning's roughness coefficient; users defined value, movable bed roughness formula of Wu and Wang (1999) and that of Van Rijn (1996). The formulas can be applied to steady or unsteady flow boundary conditions. The developers at NCCHE state that the model is developed for application to the study of unsteady, turbulent, free surface open channel flow and sediment transport problems in channels with highly irregular topography (Jia and Wang, 2001b). CCHE2D is well suited to application to the CCSB for a number of reasons:

1. the model strictly enforces mass conservation, a property that leads to more reliable and accurate results.
2. the model is capable of representing transience in the flow and sediment boundary conditions for multiple inlets and outlets
3. wetting and drying of the simulated domain is represented
4. the model can simulate mixed flow, representing both subcritical and supercritical flow in a channel reach.
5. secondary flow in bends affects direction of bed shear and mean flow; the sediment module includes the curvature effects for enhanced representation of sediment transport in bends.
6. bed roughness is updated within the model as simulations progress, to account for the effect of sediment grain size and bed form on bed roughness.

### *3.2 Third-party Calibration and Validation*

Calibration and validation simulations performed by numerous authors reinforce the applicability of the CCHE2D model to the CCSB.

### 3.2.1 NCCHE Calibration and Validation

Model developers at NCCHE present a series of verification tests for flow and sediment transport in the technical report, *CCHE2D Verification and Validation Tests Documentation* (Jia and Wang, 2001b). The following examples, all referenced from the technical report, are based on cases of analytical solution, physical model data, and natural open channel flow.

Flow in a channel with sudden expansion was simulated with CCHE2D. Simulation results were compared to velocity measurements taken during physical experiments performed by Xie (1994). Experiments were conducted for two different flow magnitudes, in a concrete flume whose dimension and flow recirculation pattern are shown in Figure 3.1. Table 3.1 contains the physical and flow parameters for each of the two test cases. Velocity measurements were taken for each flow magnitude at 11 cross sections in the experimental flume. As is seen in Figure 3.2, measured and simulated velocities correspond well, and CCHE2D performs well simulating this complicated 2-dimensional flow field. At the end of the training channel, there is a sudden expansion to the Settling Basin, which makes this problem relevant to modeling of 2-dimensional flow in CCSB.

Table 3.1 Flow conditions for the sudden expansion channel experiments conducted by Xie (1994) and simulated by Jia and Wang, (2001b).

| Discharge ($m^3/s$) | Width (m) | Depth (m) | Step Height (m) | Slope | Approach Main Velocity (m/s) | Approach Froude Number | Recirculation Length (m) |
|---|---|---|---|---|---|---|---|
| 0.01815 | 1.2 | 0.101 | 0.6 | 1/1000 | 0.30 | 0.30 | 4.60 |
| 0.03584 | 1.2 | 0.105 | 0.6 | 1/1000 | 0.60 | 0.60 | 4.60 |

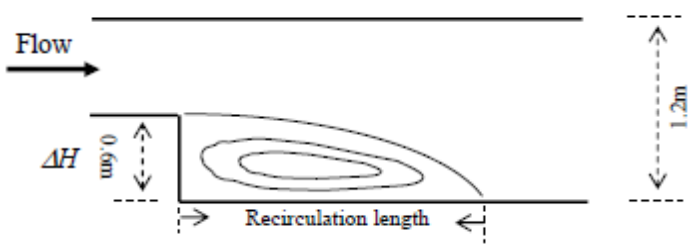


Figure 3.1. Flume dimension and recirculation pattern of Xie (1994) experiments (from Jia and Wang, 2001b)

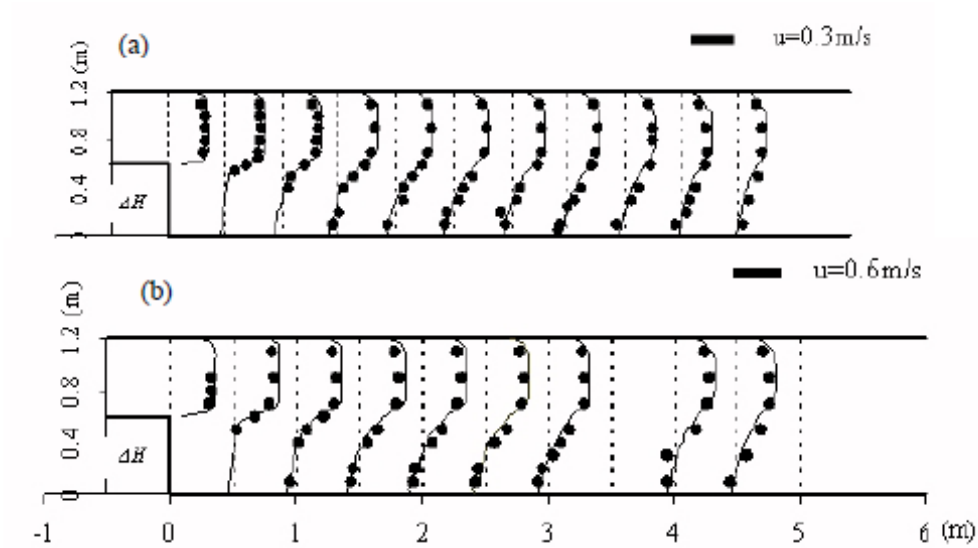


Figure 3.2 Comparisons of the simulated (line) and measured (circles) flow field in the channel of sudden expansion, a: Q=0.01815m$^3$/s, b: Q=0.03854m$^3$/s (Jia and Wang, 2001b)

Flow in a 180-degree U-shaped channel, representative of severe meander was also presented in the manual. The developers simulated physical experiments originally conducted by De Vriend (1979). Again, comparisons of detailed horizontal velocities were made at many cross sections along the simulated channel length. Flow and physical parameters are tabulated in Table 3.2, while the simulation mesh, and velocity comparisons are shown in Figure 3.3 and 3.4 respectively. Once more, the 2-dimensional flow field is well simulated as experimental and simulated water velocities match closely.

Table 3.2 Flow conditions for the 180-degree U-shaped channel, (from Jia and Wang, 2001b).

| Discharge (m$^3$/s) | Width (m) | Depth (m) | Slope | Mean Velocity (m/s) | Reynolds Number | Froude Number |
|---|---|---|---|---|---|---|
| 0.180 | 1.7 | 0.1953 | 0 | 0.542 | 1513 | 0.392 |

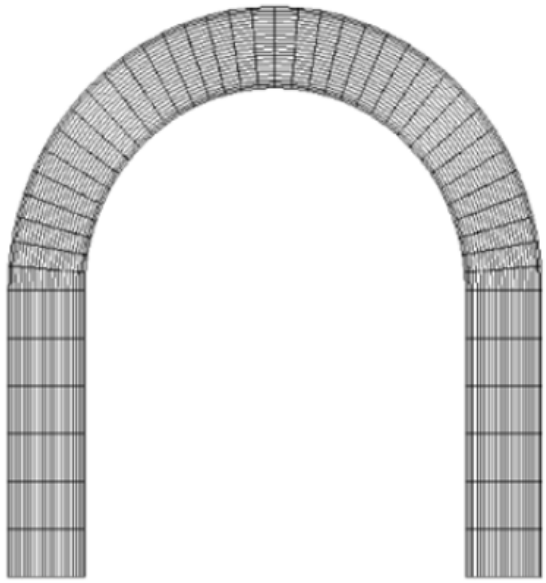

Figure 3.3 Mesh system of the 180-degree U-shaped channel (Jia and Wang, 2001b)

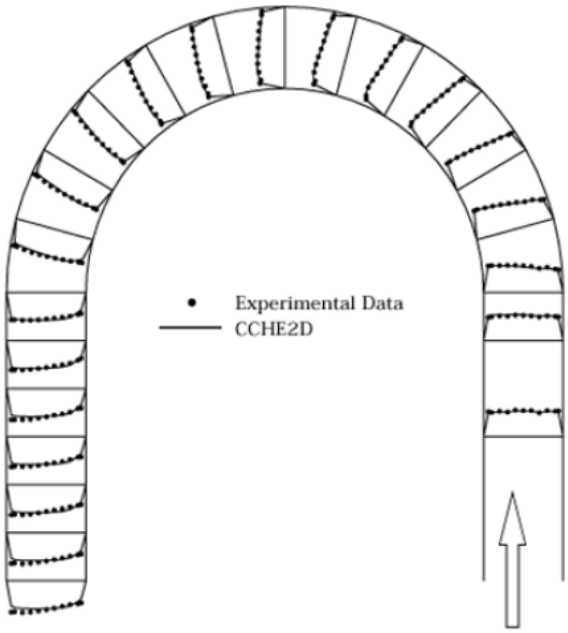


Figure 3.4 Simulated and measured velocities of the 180-degree U-shaped channel (Jia and Wang, 2001b)

The final verification of CCHE2D's flow modeling capability is highly applicable to the CCSB, as it compares flow field simulations of a compound channel to velocity measurements in an experimental flume. In this experimental case, there is a main flow channel with a flood plain on one side of the channel only. A definition sketch is shown in Figure 3.5. Experimental parameters of the physical experiment conducted by Rajaratnam and Ahmadi (1981) are shown in Table 3.3. Flow comparisons of the experimental measurements to three different

simulation results, which varied the eddy viscosity coefficient and boundary slip coefficient are presented in Figure 3.6. The results improve with adjustment of the boundary slip coefficient, and provide verification that the model performs well in representing flow fields in compound channels.

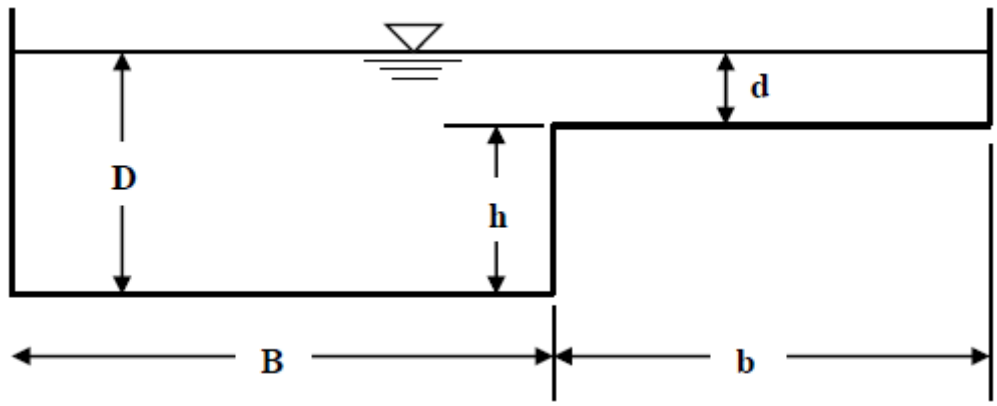


Figure 3.5 Definition sketch of the compound channel components (Jia and Wang, 2001b)

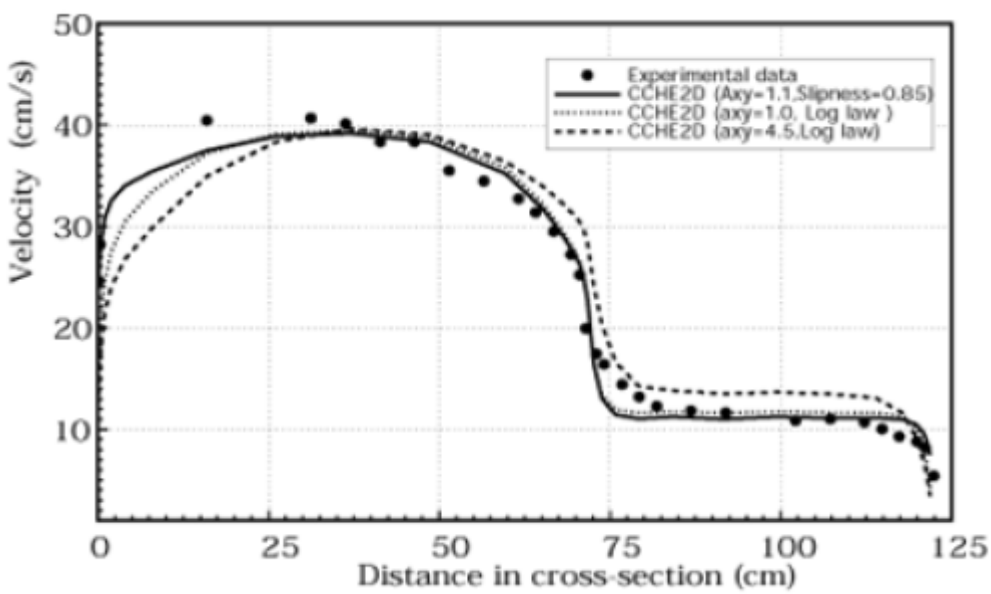


Figure 3.6 Comparison of measured and simulated velocity in a compound channel (Jia and Wang, 2001b)

Table 3.3 Parameters of the compound channel experiment (Jia and Wang, 2001b).

| D (cm) | d (cm) | h (cm) | B (cm) | b (cm) | Discharge ($m^3/s$) |
|---|---|---|---|---|---|
| 11.28 | 1.52 | 9.75 | 71.1 | 50.8 | 0.027 |

Sediment transport verification was presented in the manual for cases of bed aggradation and degradation by comparing simulation results to flume experiment results, and suspended sediment transport in a meandering river was simulated and compared to field measurements in the River Nechar, in Germany.

A flume experiment of channel aggradation conducted by Soni (1981) was simulated based on the flow and sediment conditions given in Table 3.4. Results of the simulation and experiment are presented in Figure 3.7, in which bed elevation is presented at thirty-minute intervals through the experiment. The trend of bed elevation increasing with time is clear and the agreement between simulated and experimental values is clear.

Table 3.4 Sediment and initial flow conditions, bed aggradation experiment performed by Soni (1981) (from Jia and Wang, 2001b).

| Unit Discharge ($m^2/s$) | Mean velocity (m/s) | $d_{50}$ (m) | Bed Roughness (m) | Depth (m) | Bed Slope | Froude Number |
|---|---|---|---|---|---|---|
| 0.0355 | 0.493 | 0.0003 | 0.022 | 0.072 | 0.00427 | 0.34 |

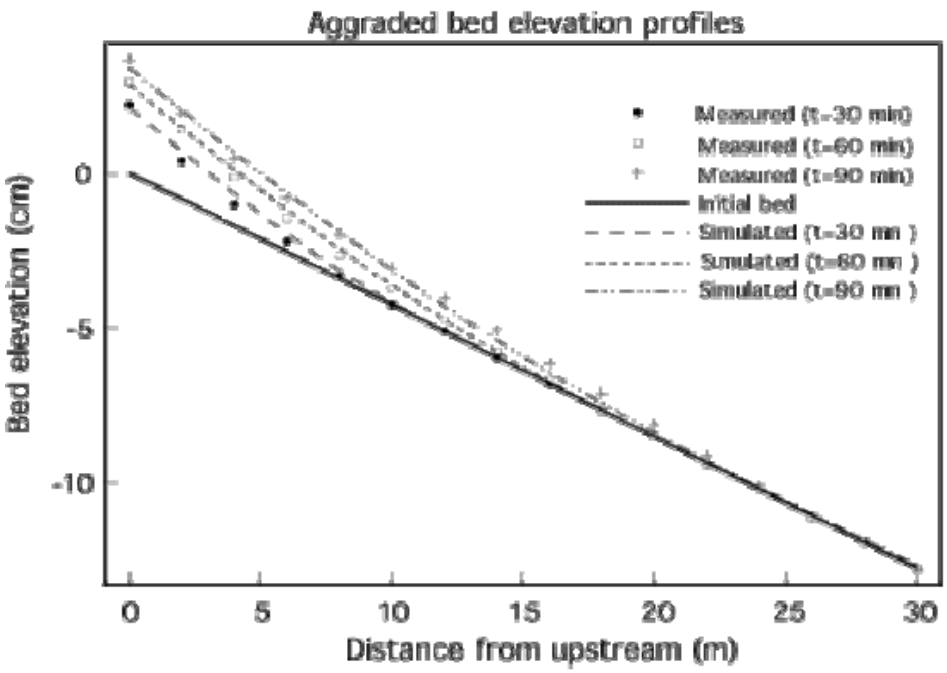


Figure 3.7 Comparison of measured and simulated bed elevations, bed aggradation experiment (Jia and Wang, 2001b)

A flume experiment of bed degradation conducted by Newton (1951) was simulated, based on the conditions given in Table 3.5. The simulations for bed degradation were conducted using the Van Rijn bed roughness model, one of the two bed roughness models applicable in the CCHE2D model. Additionally, the non-equilibrium sediment transport relationship selected for application in this case is the Bell-Sutherland relation. These selections are described in more detail in Jia and Wang (2001a). The bed degradation results for the experiment and simulation are compared in Figure 3.8. Experimental bed elevation was measured every hour through a 24-hour experiment, and simulated results are plotted to compare to reported experiment results at t = 1, 2, 3, 4, 5 and 24 hours.

Table 3.5 Sediment and initial flow conditions, bed degradation experiment performed by Newton (1951) (from Jia and Wang, 2001b).

| Unit Discharge ($m^3/s$) | Mean Velocity (m/s) | $d_{50}$ (m) | Bed Roughness (m) | Bed Slope | Froude Number |
|---|---|---|---|---|---|
| 0.0185 | 0.45 | 0.00069 | 0.041 | 0.00416 | 0.50 |

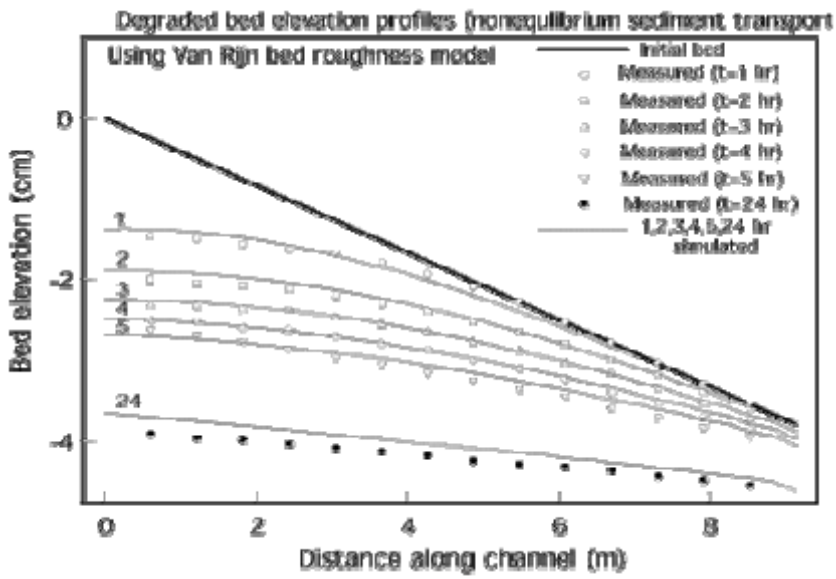


Figure 3.8 Comparison of experimental and simulated results, bed degradation experiment (Jia and Wang, 2001b)

The River Nechar, in Germany is a natural river channel with a complicated geometry consisting of sharp bends and wider flood plains. Suspended sediment concentration was measured by Xu et al. (2001) along several cross sections of the natural river, and compared to CCHE2D unsteady flow and sediment simulations of the river system performed by the model developers. Figure 3.9(a) provides a contour plot of suspended sediment concentration for the simulated system. The solid blue areas represent the flood plains, and the cross sections used for comparison are marked in the figure. Comparisons of the suspended sediment concentrations are shown in Figure 3.9(b). Correspondence of measured and computed sediment concentration is similar in each cross section, regardless of distance from the inlet boundary, and along each cross section regardless of the distance from the bank. CCHE2D predicts the suspended sediment concentration well in both the lateral and longitudinal directions.

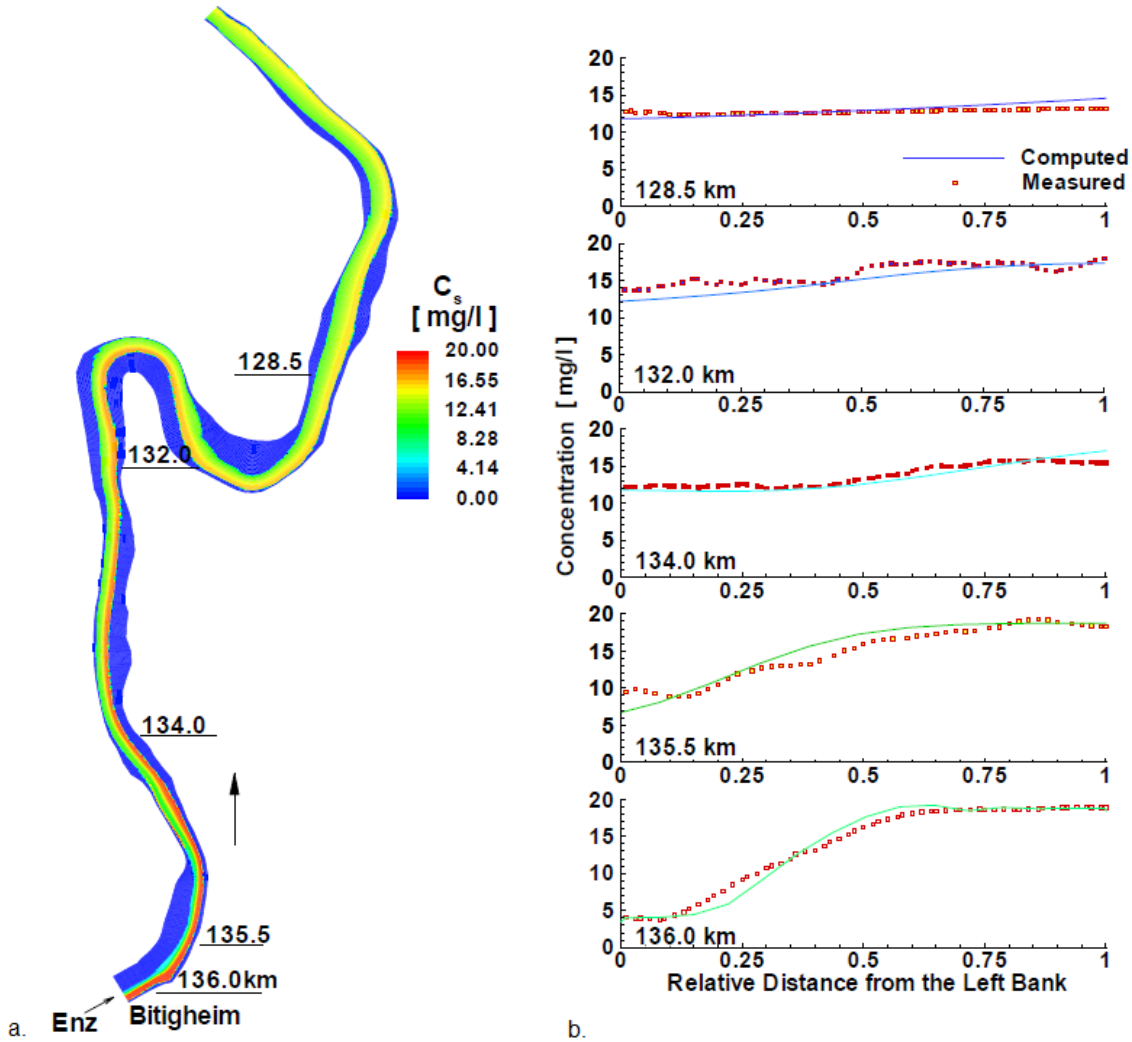


Figure 3.9. Suspended sediment verification results, River Nechar, Germany: a. sediment concentration contour plot; b. comparison of measured and computed sediment concentrations (Jia and Wang, 2001b)

### 3.2.2 Non-Principal Calibration and Validation

A number of investigations have been performed by parties unaffiliated with the development of CCHE2D to verify use of CCHE2D as a 2-dimensional flow and sediment transport model. A select group is presented here as their findings support the application of CCHE2D to the CCSB.

Kantoush et al. (2008) studied the influence of reservoir geometry on flow pattern and sedimentation, focusing on shallow rectangular reservoirs. The authors aimed to compare the abilities of ultrasonic doppler velocity profilers (UVP), large-scale particle image velocimetry (LSPIV), and numerical simulation by CCHE2D to create a 2-dimensional flow field representation. They conducted lab experiments in which detailed velocity measurements were taken to map the flow field in a shallow reservoir model. Although the study involved

sedimentation patterns, the authors did not present results comparing sediment transport in the model with simulations using CCHE2D. The experiments involved low flow velocities and reservoir geometry that created recirculation and eddies in the reservoir interior, as is expected in portions of the CCSB. Comparison of velocity maps produced from UVP, LSPIV, and CCHE2D are presented in Figure 3.10. CCHE2D can represent the recirculating flow pattern measured and created in the experimental reservoir.

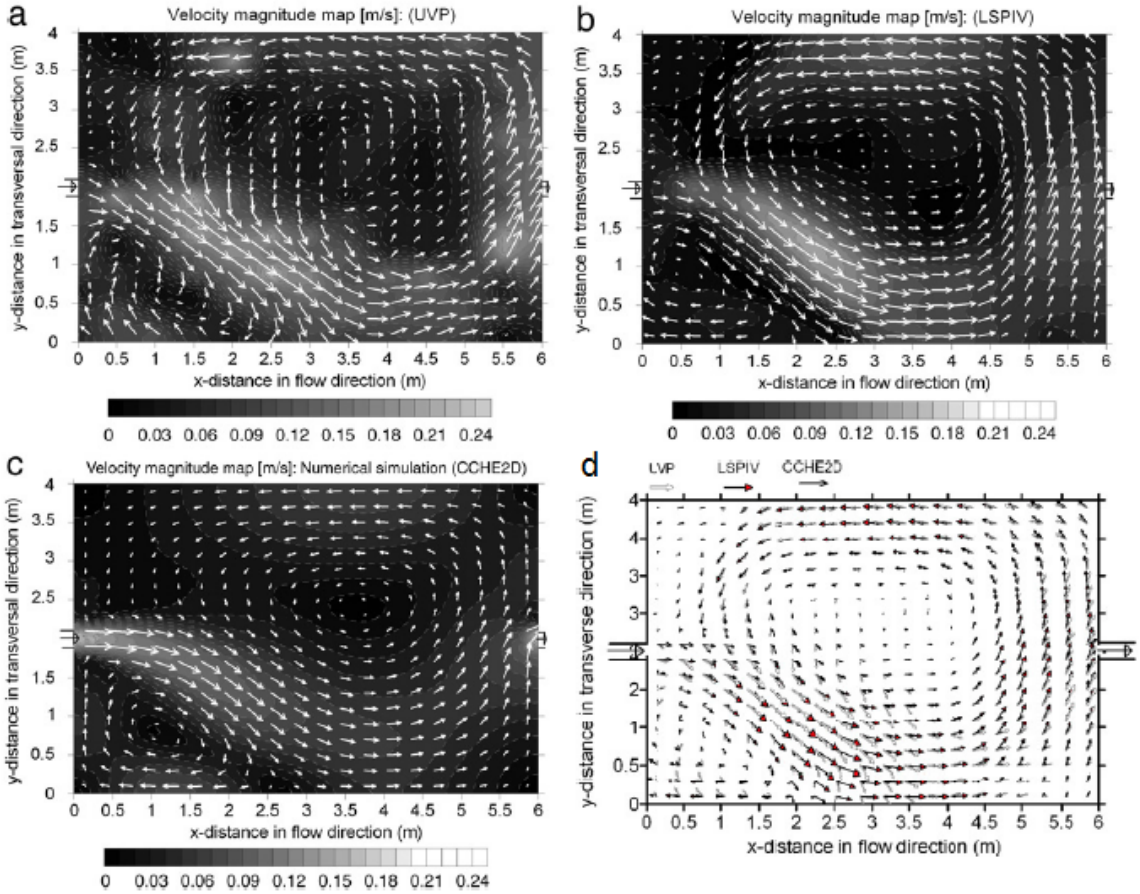


Figure 3.10 Flow field from (a) UVP (b) LSPIV (c) CCHE2D and (d) comparison of velocity magnitude vectors obtained from all three methods

Mohanty et al. (2012) conducted a study to investigate flow in a wide meandering compound channel. Physical experiments were conducted using a sinusoidal river with trapezoidal main channel and wide flood plains on either bank (Figure 3.11). Five experimental runs were conducted with different discharge magnitudes and overbank depths as tabulated in Table 3.6. Experimental values of velocity and boundary shear distribution for each run were then compared to CCHE2D simulation results, and Conveyance estimation System model results for each of the five experiments. Simulated results of normalized velocity are shown in Figure 3.12. CCHE2D measurements agree so well with the experimental measurements, the two are difficult to distinguish in the figure. Comparisons of shear stress are displayed in Figure 3.13, and again the match

between CCHE2D results and measured values is quite good. The authors conclude that CCHE2D is a "viable research tool in the field of river engineering".

Table 3.6 Hydraulic parameters for the experimental runs, meandering compound channel (Mohanty et al., 2006).

| Sl. no. of Runs | *Discharge Q in lit/s | Overbank depth H in cm | Relative depth β(H-h/H) | Froude no.(Fr) | Reynolds no.(R) |
|---|---|---|---|---|---|
| 1 | 17.074 | 8.06 | 0.19354839 | 0.2199681 | 19681.77 |
| 2 | 27.617 | 8.55 | 0.23976608 | 0.28274994 | 27641 |
| 3 | 47.245 | 9.5 | 0.31578947 | 0.33944679 | 38865.04 |
| 4 | 70.338 | 10.2 | 0.3627451 | 0.40923323 | 52128.25 |
| 5 | 93.667 | 11 | 0.40909091 | 0.4432553 | 63233.17 |

*---Discharges as per measured from contour diagram

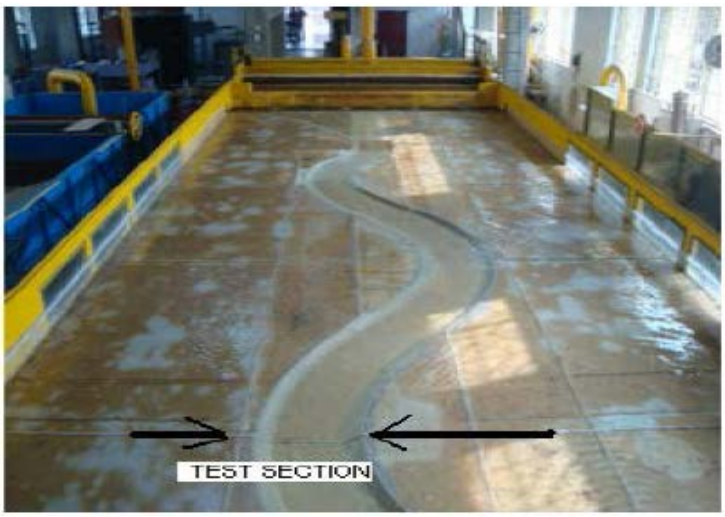


Figure 3.11 Experimental set-up for meandering compound channel Mohanty et al. (2012)

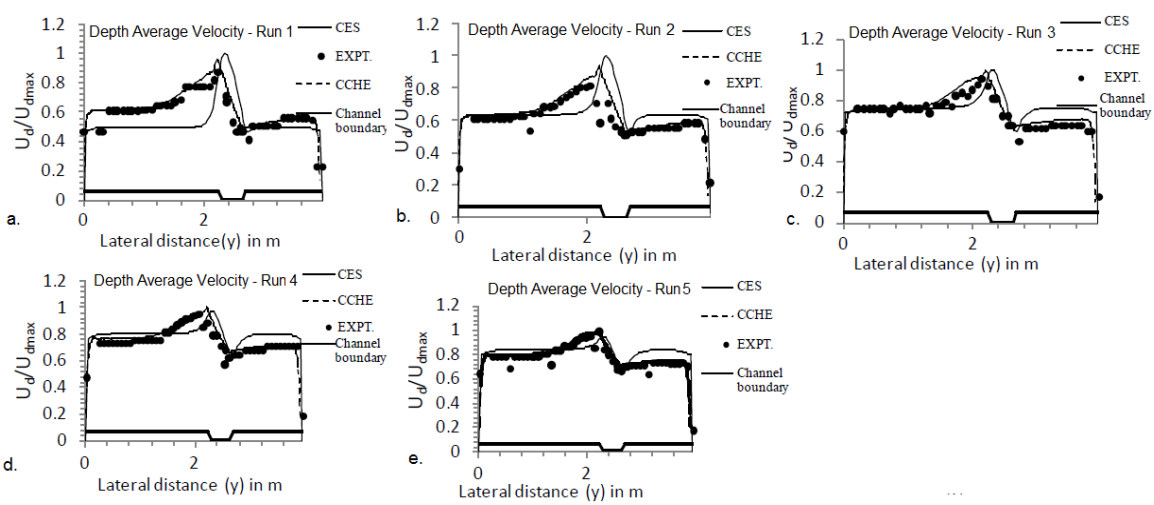


Figure 3.12 Normalized depth averaged velocity diagrams for each of the five runs (a) Run 1 (b) Run 2 (c) Run 3 (d) Run 4 (e) Run 5 (Mohanty et al., 2012)

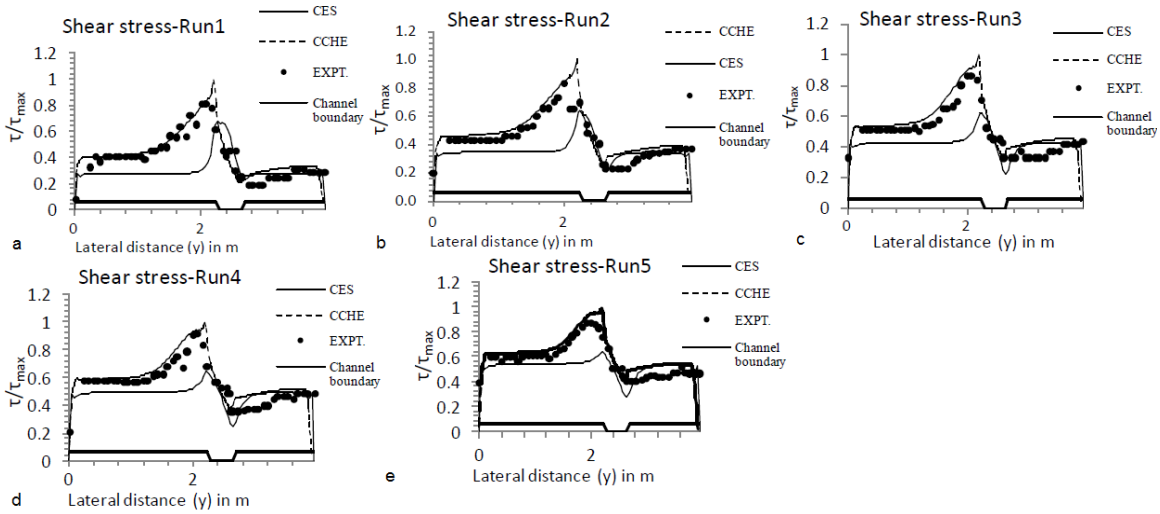


Figure 3.13 Shear velocity diagrams for each of the five runs (a) Run 1 (b) Run 2 (c) Run 3 (d) Run 4 (e) Run 5, (Mohanty et al., 2012)

Investigations into the capability of CCHE2D to represent sediment transport, erosion and deposition have been undertaken as well. Huang (2007) is an example of the complexities of sediment transport modeling. The author investigated the effects of the five different sediment transport formulae; Wu et al. (2000) bed-load formula, Wu et al. (2000) bed-material load formula, Modified Ackers–White bed-material formula, Modified Engelund–Hansen bed-material load formula and SEDTRA module for bed-material load, and the three methods for estimating Manning's roughness coefficient: users defined value, movable bed roughness formula of Wu and Wang (1999) and that of Van Rijn (1996), which are available in CCHE2D for both steady and unsteady flow boundary conditions. As the results for unsteady flow conditions are relevant to the work presented herein, they alone are presented. Figure 3.14 contains plots comparing experimentally measured bed degradation data to the simulation results for the 15 possible combinations. The author concludes that not only is a moveable bed roughness formula needed in sediment transport modeling, but that testing of the transport formulae is significantly needed in order to find the best formula for each application.

Negm et al. (2010) utilized CCHE2D to study the scouring and silting processes in the Sudanese portion of the High Aswan Dam Reservoir in an effort to determine the reservoir's life span. Their CCHE2D representation of the reservoir was calibrated and verified with field data, and applied to predict cross sections along the reservoir for 2010, 2020, 2030 and 2040. Calibration results for bed level prediction of two cross sections are displayed in Figure 3.15. Verification results for bed level prediction of two cross sections are displayed in Figure 3.16. The verification results are a good fit to measured bed elevation, as can be seen in Figure 3.17. The plot shows a 1:1 correspondence line, with model data plotted versus measured data in which a perfect fit would lay directly on the 1:1 line. Divergence in measured and modeled results is small enough for

the authors to conclude that CCHE2D can be used as a long-term predictor of bed elevation change, and ultimately reservoir life time span.

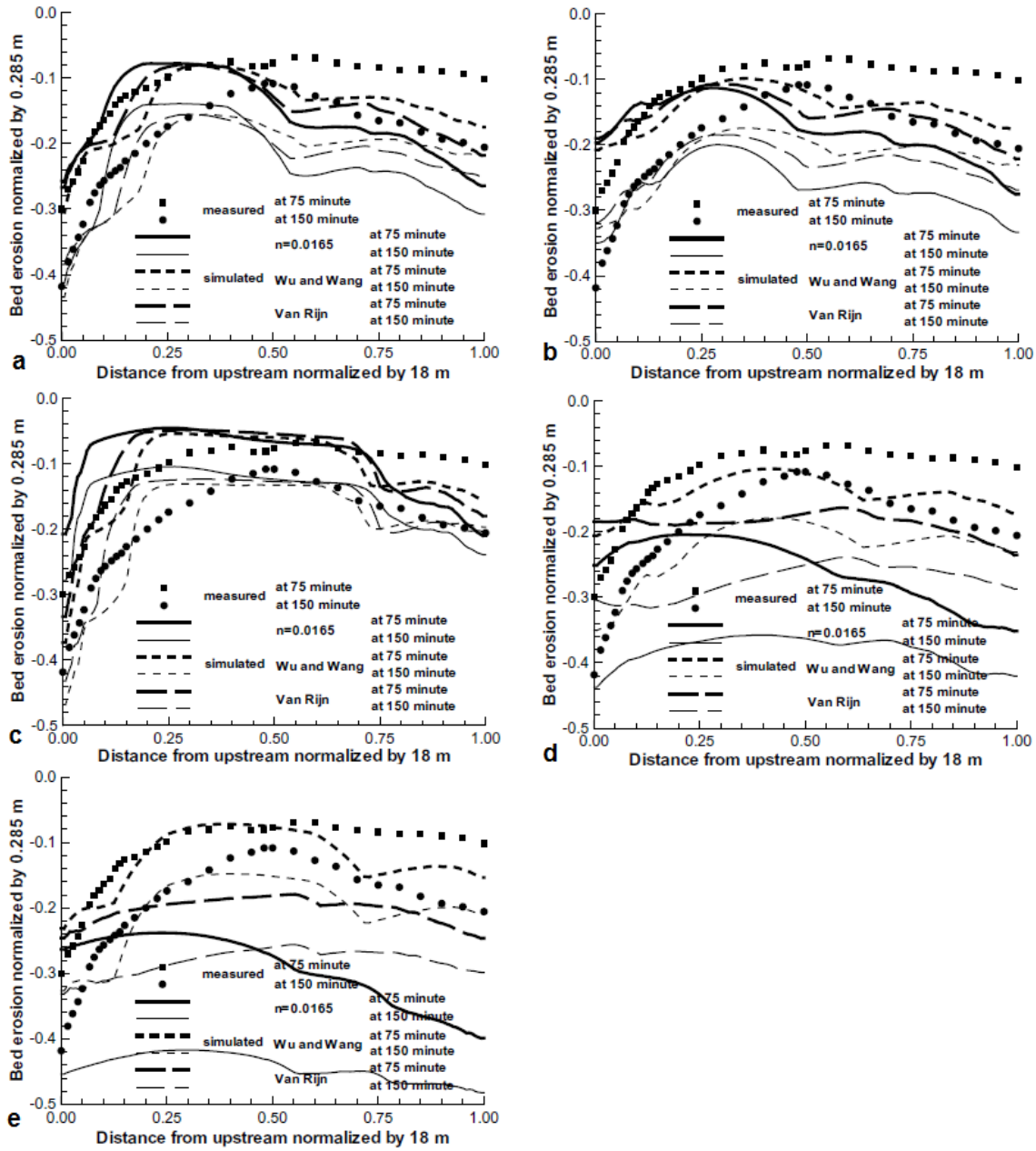


Figure 3.14 Huang (2000) Channel degradation comparison, utilizing each bed roughness method for (a) Wu et al. (2000) bed-load formula, (b) Wu et al. (2000) bed-material load formula, (c) Modified Ackers–White bed-material formula, (d) Modified Engelund–Hansen bed-material load formula and (e) SEDTRA module

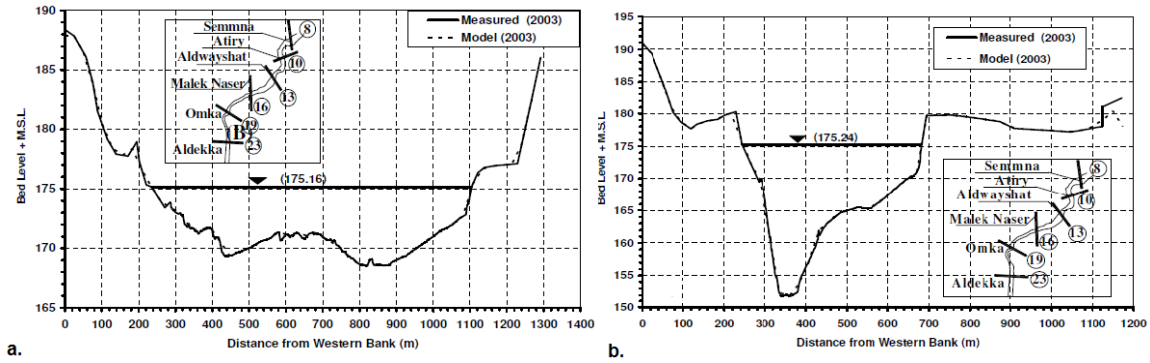


Figure 3.15 Calibration results for cross section bed level in 2003 (a) section 13 and (b) section 16 (Negm et al., 2010)

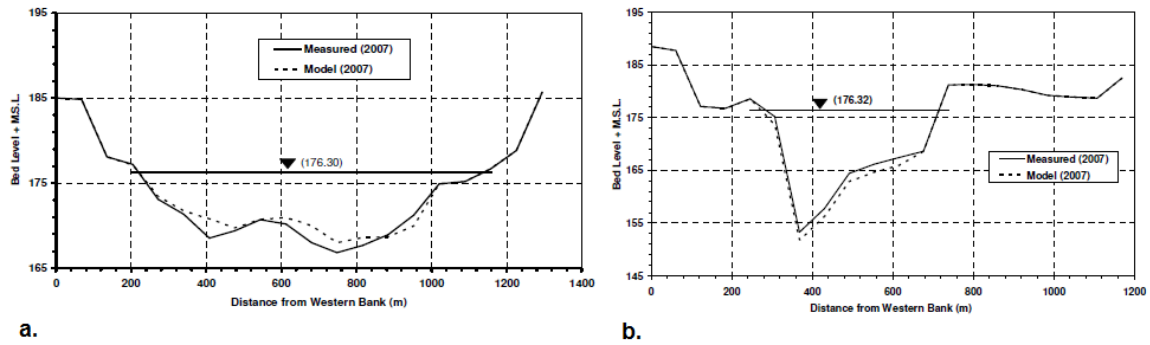


Figure 3.16 Verification results for cross section bed level in 2007 (a) section 13 and (b) section 16 (Negm et al., 2010)

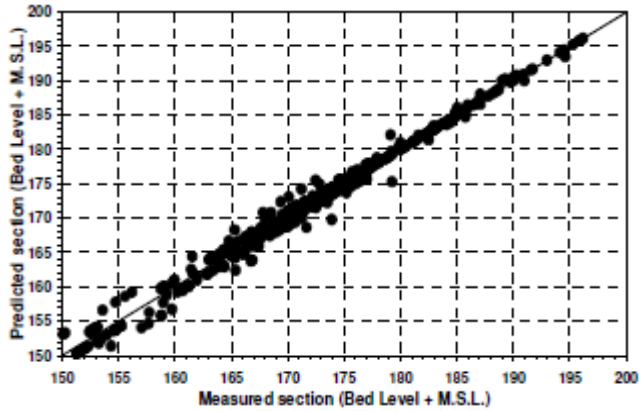


Figure 3.17 Predicted bed elevation for sections 13 and 16 plotted against corresponding measured bed elevation (Negm et al., 2010)

## 4 CCHE2D FLOW SIMULATIONS

Numerical simulations of the river and basin from Cache Creek at Yolo to the outlets of the CCSB were initiated, calibrated and validated for observed flows up to 15,000 cfs. Mesh generation is the initial step in simulating flow and sediment transport, and is an integral and time consuming component of successful numerical simulation. In order to adequately describe the topography, and accurately represent the hydrodynamics of the CCSB a dense mesh was created, which optimized accuracy without sacrificing computational time required for each simulation. It is not realistic to use Road 102 as the upstream boundary condition for the CCSB simulations as there is limited flow data.

Therefore, the simulation area of the CCHE Settling Basin model was extended to include Cache Creek at Yolo where there exists a long-standing 15-minute flow record. Moreover, a considerable number of sediment measurements with concurrent flow measurements are also available at Cache Creek at Yolo. The simulation mesh of the extent from Cache Creek at Yolo to Rd 102 is shown in Figure 4.1. The simulation mesh for the CCSB is shown in Figure 4.2. The computational domain is composed of about 15,400 computational nodes from Cache Creek at Yolo to Road 102 and about 60,013 computational nodes from Road 102 to overflow weir. The total number of nodes is more than 75,000 for the entire computational domain. The complex bathymetry and the flow dynamics in the training channel and in the Settling Basin make it necessary to have such dense computational nodes. The mesh is sufficiently dense that visualization of the full extent is difficult, and a magnified region is shown in each figure. Corresponding elevation contours for the extent from Yolo to Rd 102, and the CCSB are shown in Figures 4.3 and 4.4 respectively. Figure 4.4 also contains approximate locations of the measurement stations used for calibration and validation of simulation results.

The simulations utilized inflow boundary data taken from instantaneous flow data at the Cache Creek at Yolo gauge (source: http://nwis.waterdata.usgs.gov, USGS 11452500) from March 18, 2011 through March 22, 2011. The simulations also utilized rating table boundary conditions at the overflow weir, as provided by USGS (Brazelton, W. 2010 "Rating Curve for Cache Creek Settling Basin Weir") and at the outlet culvert box of the low flow channel (source: http://nwis.waterdata.usgs.gov, USGS 11452900). The rating curve for the overflow weir is shown in Figure 4.5, and the rating curve for the low flow culvert is shown in Figure 4.6.

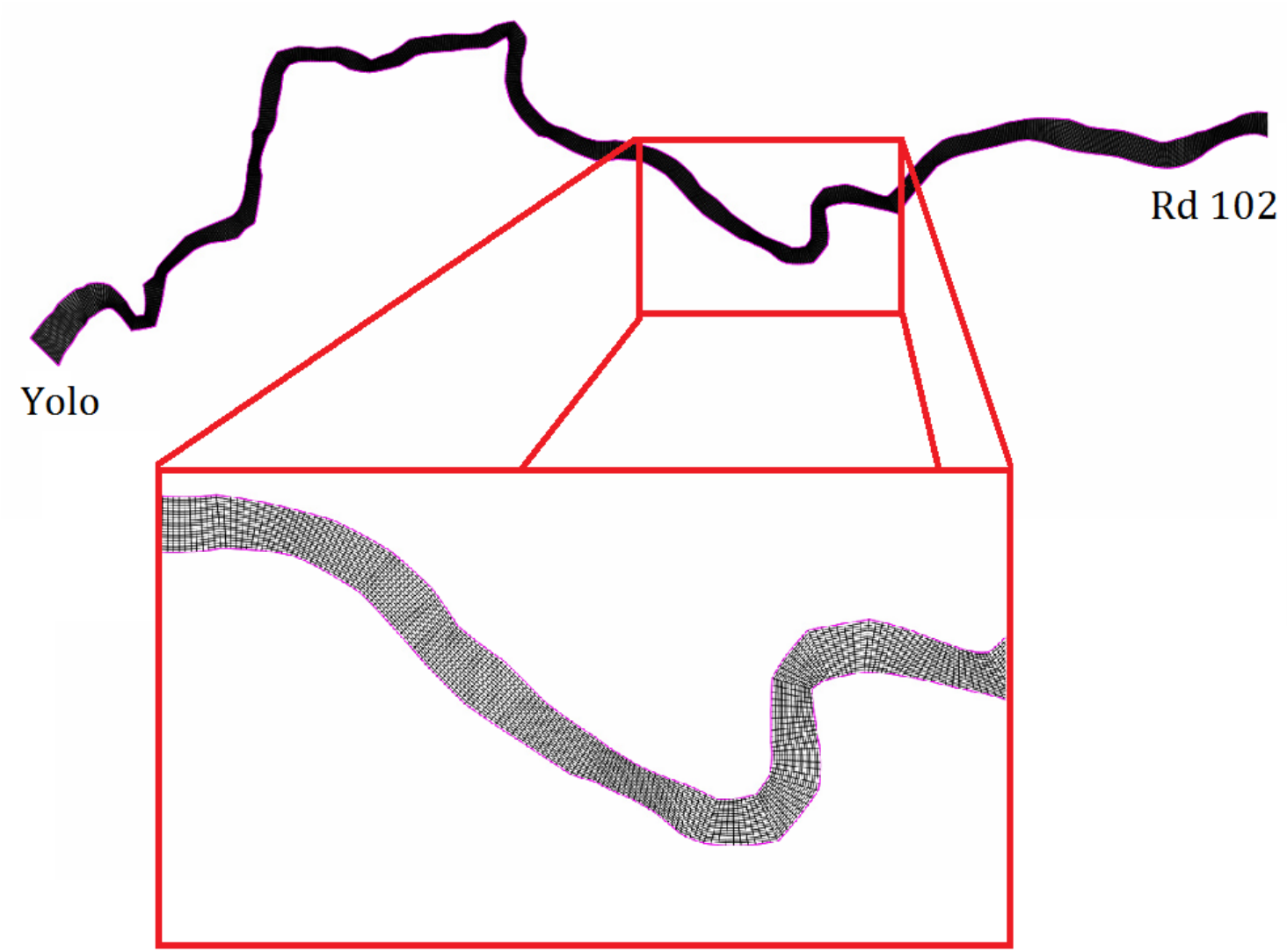


Figure 4.1 Mesh from Cache Creek at Yolo to Road 102

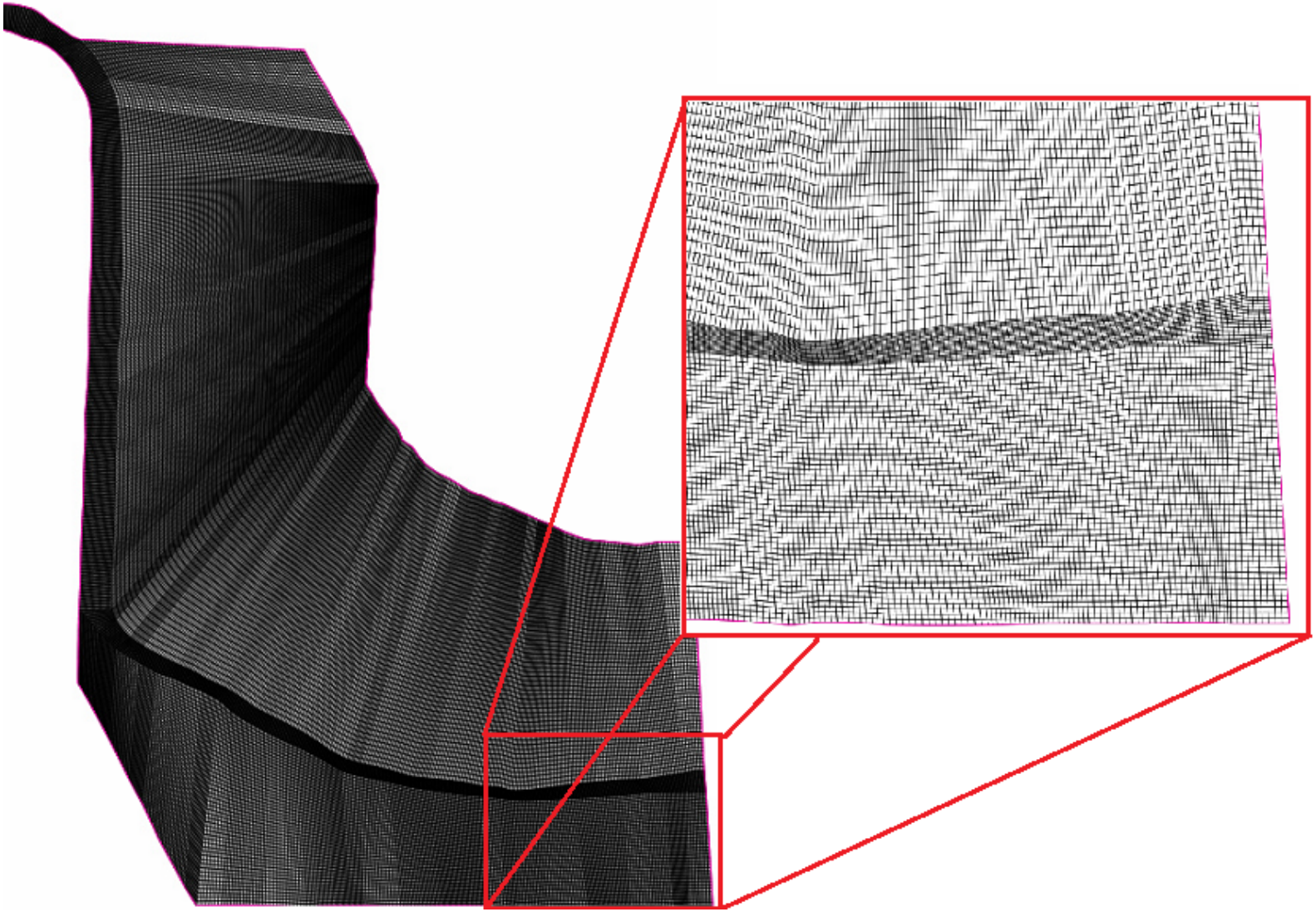

Figure 4.2 Simulation Mesh for CCSB

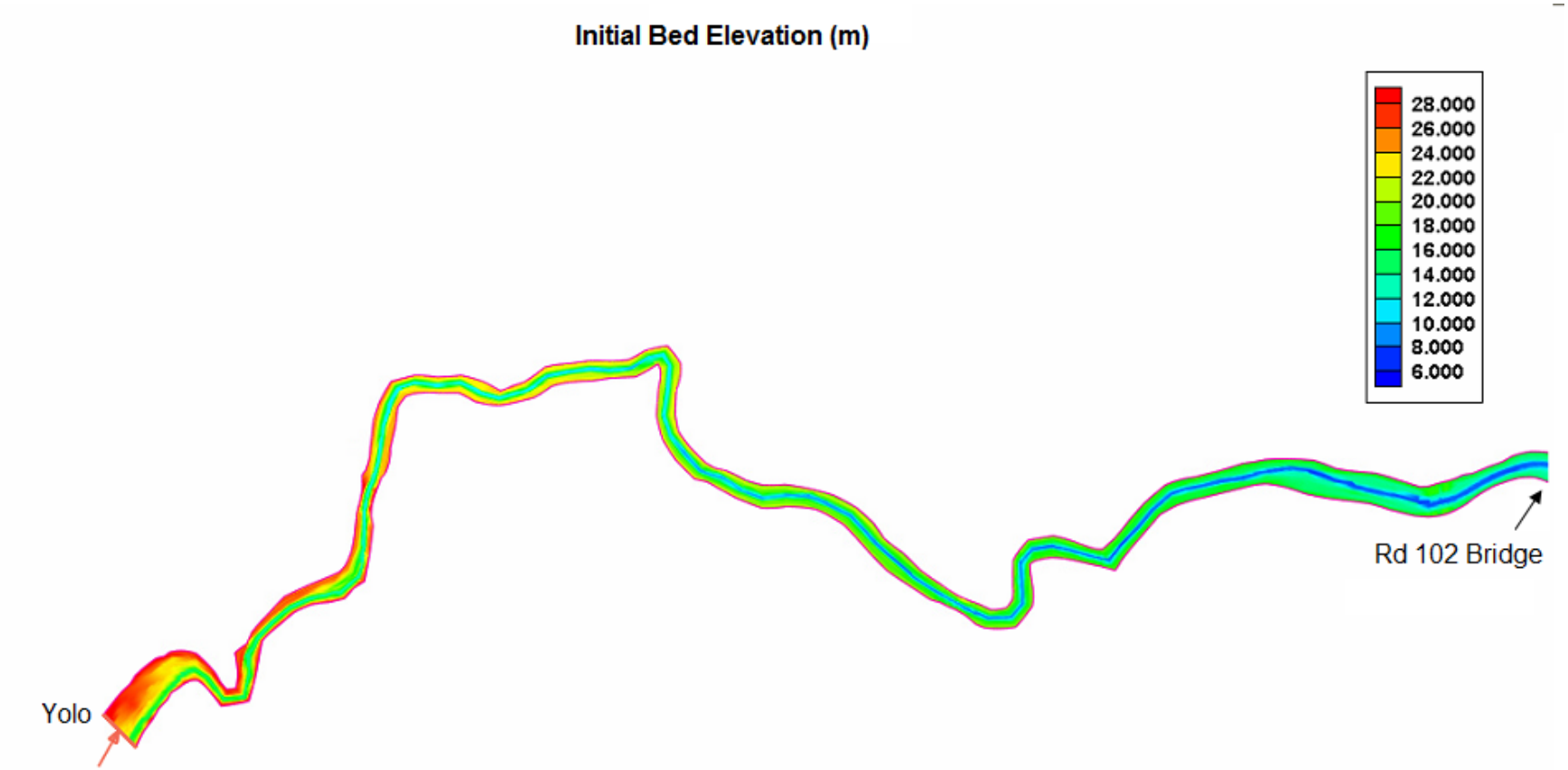


Figure 4.3 Elevation contour of simulated extent from Cache Creek at Yolo to Rd 102

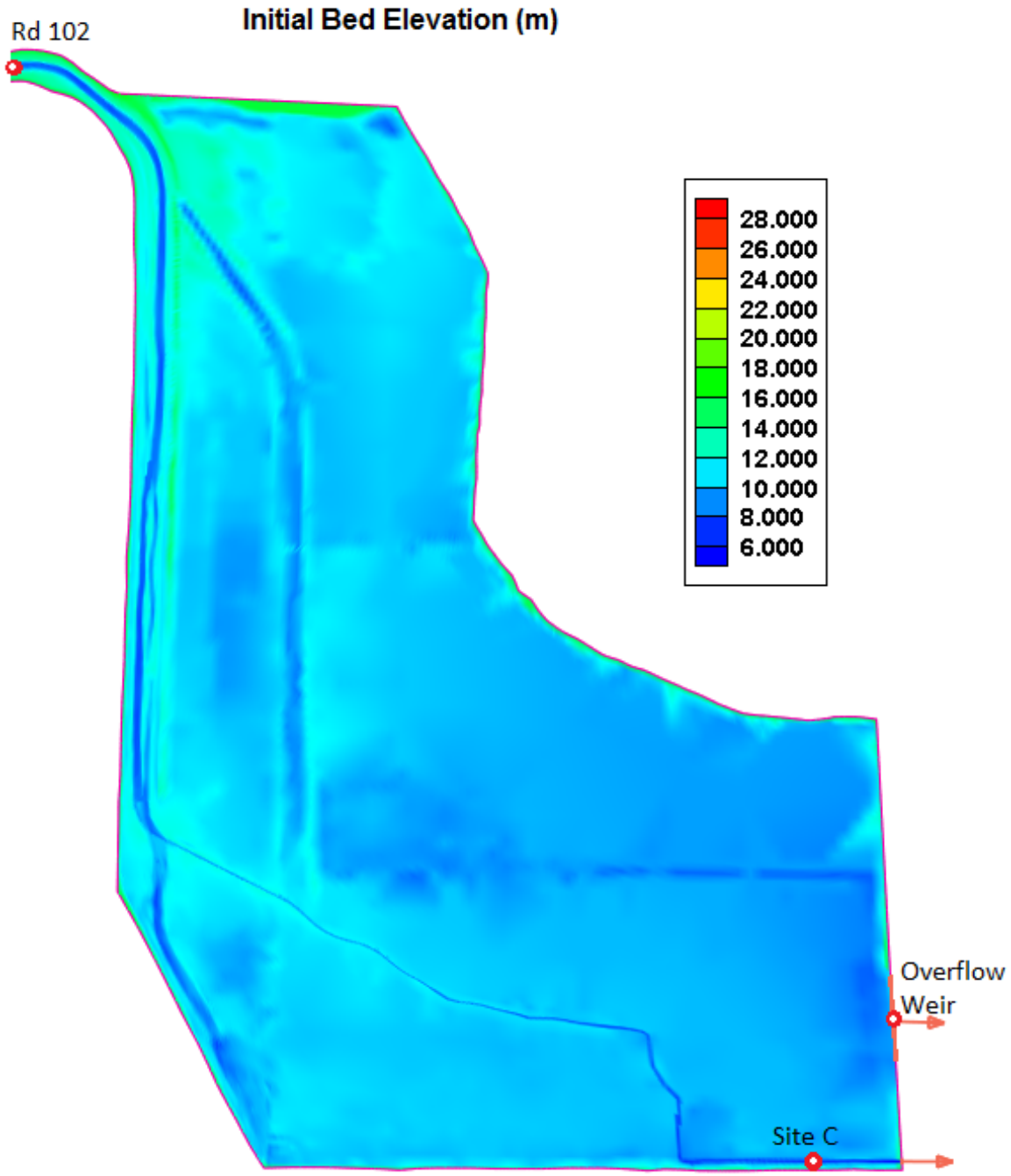


Figure 4.4 Elevation contour of simulated extent, Rd 102 through CCSB including approximate locations of result comparison points

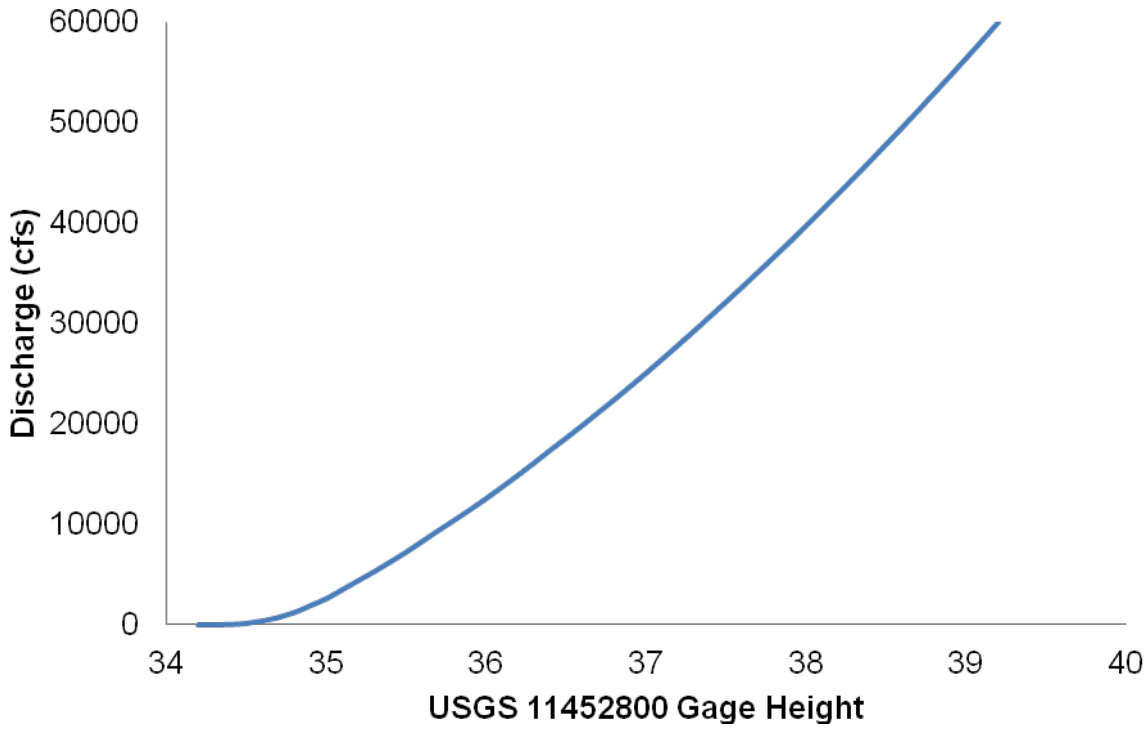


Figure 4.5 Rating curve for the USGS site 11452800, CCSB overflow weir.

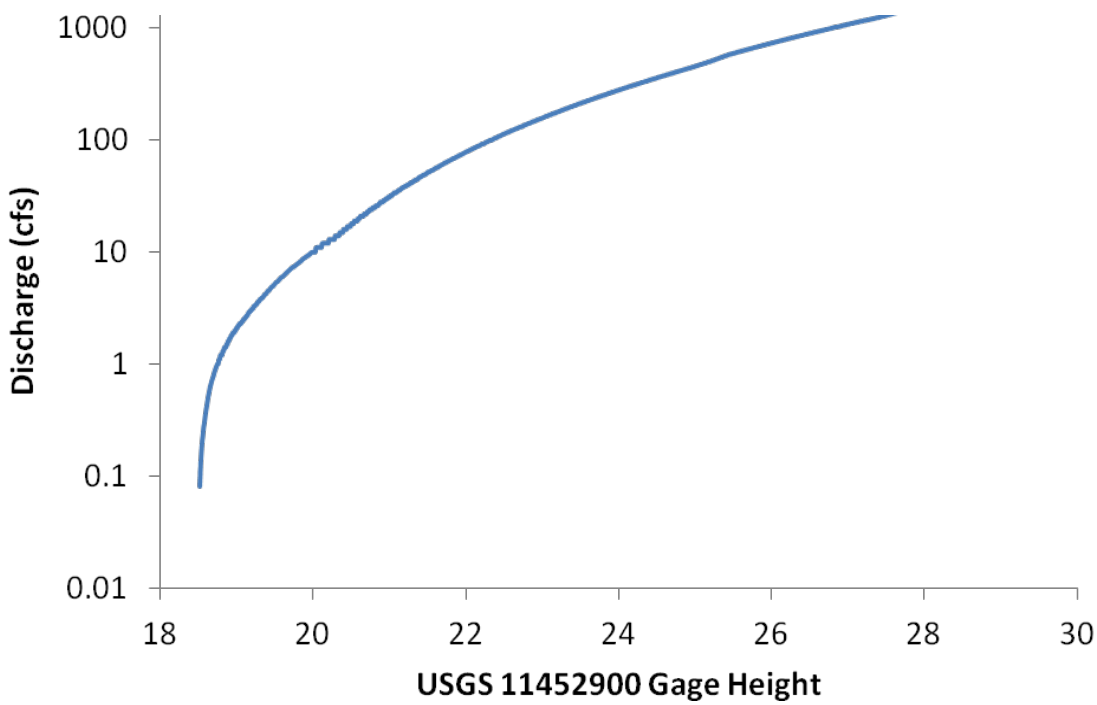


Figure 4.6 Rating curve for USGS site 11452900, CCSB low flow culvert.

### 4.1.1 Calibration by 18-22 March 2011 event at Road 102

Correct specification of parameters such as; time step, turbulence model, wall slipness, bed roughness and bed sediment grain size are essential to accurate representation of field conditions. CCHE2D requires that bed grain size distribution be defined by specifying the D16, D50 and D90 sediment sizes. As noted previously, the model also allows either user specified bed roughness, or to select one of two bed roughness formulae (Wu and Wang, 1999 and van Rijn 1986) which calculate roughness as a function of the grain size distribution.

Sensitivity analyses were performed to determine what bed roughness method and sediment grain size distribution should be applied when simulating the CCSB. Simulations were run for each of the two bed roughness formulae, and different specified values of bed roughness. Results of the simulations at Rd 102 were compared to measured water surface elevation values provided by USGS (B. Brazelton, personal communication, November 4, 2011). Water surface elevation results at Rd 102 for various bed roughness methods are presented in Figure 4.7, along with the USGS data. Figure 4.7 also contains a plot of the percent error for each bed roughness method. The Wu and Wang (1999) solution of bed roughness has been selected for application to the CCSB as it provides the highest level of agreement between the simulated and measured water data. Using a constant roughness value for all flow conditions is not realistic for the Settling Basin's dynamic flow conditions. Moreover, bed elevation is changing due to deposition and erosion in the Settling Basin. The roughness formula of Wu and Wang (1999) considers flow and bed elevation change and utilizes a more realistic roughness value considering the Froude number at each grid node.

Once identified as the most suitable bed roughness method, the Wu and Wang (1999) formula was tested with three different grain size specifications, to identify sensitivity to grain size and to calibrate model roughness. The three different distributions of grain size, denoted A, B and C, are presented in Table 4.1. Simulation results of water surface elevation at Rd 102 corresponding to these parameters are plotted in Figure 4.8, along with the measured data. The percent error for simulation results for each of the grain size distributions is also plotted in Figure 4.8, and it can be observed that distribution B performs the best.

Table 4.1 Grain size distributions applied with Wu and Wang (1999) roughness simulations.

| | Grain Size Distribution | | |
|---|---|---|---|
| | A | B | C |
| D16 (mm) | 0.127 | 0.254 | 1.270 |
| D50 (mm) | 0.286 | 0.572 | 2.861 |
| D90 (mm) | 2.293 | 4.585 | 22.926 |

The normalized root mean square errors for the best performance trials of each bed roughness method are tabulated in Table 4.2. The normalized root mean

square error $\left( NRMSE = \sqrt{\frac{\sum_{i=1}^{n}\left(x_{1,i} - x_{2,i}\right)^2}{n\left(x_{1,max} - x_{1,min}\right)^2}} \right)$, where $x_1$ are the measured values, $x_2$ are the modeled values, and n is the number of time steps evaluated, is used to aid in comparison of each case. Its value indicates the level of agreement between the measured and modeled values. The lower the NRMSE, the less variance there exists in the difference of the model and measured values over all time steps.

The CCHE model utilizing Wu and Wang (1999) bed roughness method with grain size distribution B in Table 4.1 is selected as the best solution through the calibration process, and is validated for 18-22 March 2011 flow event by observed water elevations at site C and overflow weir. Moreover, the entire CCHE model of CCSB is validated for 23-27 March 2011 flow event by the observed water elevations at three locations: Road 102, site C and overflow weir.

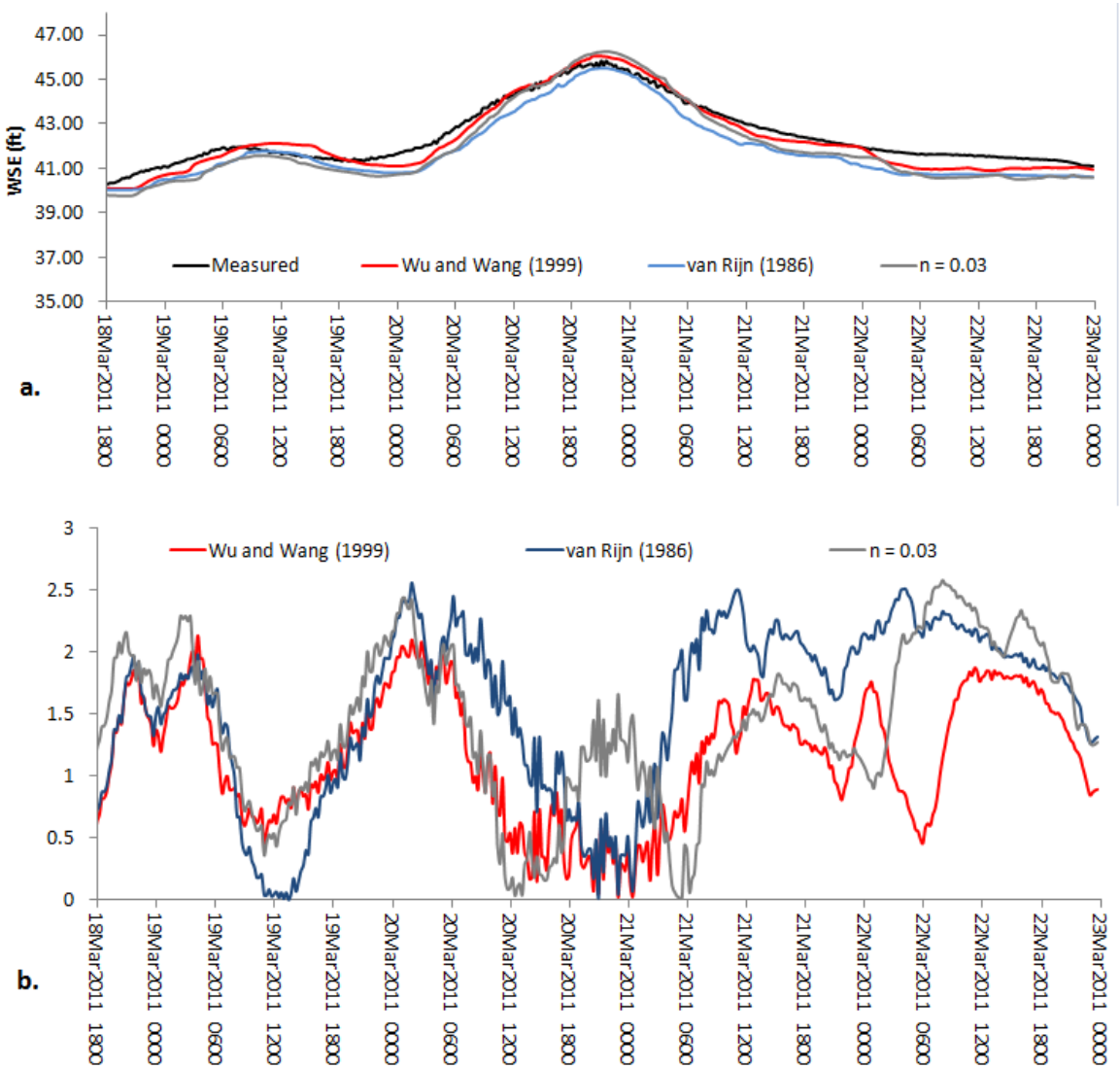


Figure 4.7 (a) Results of CCHE2D water surface elevation at Rd 102 for various bed roughness and measured water surface elevation at Rd 102, and (b) percent error of simulated water surface elevations for various bed roughness methods

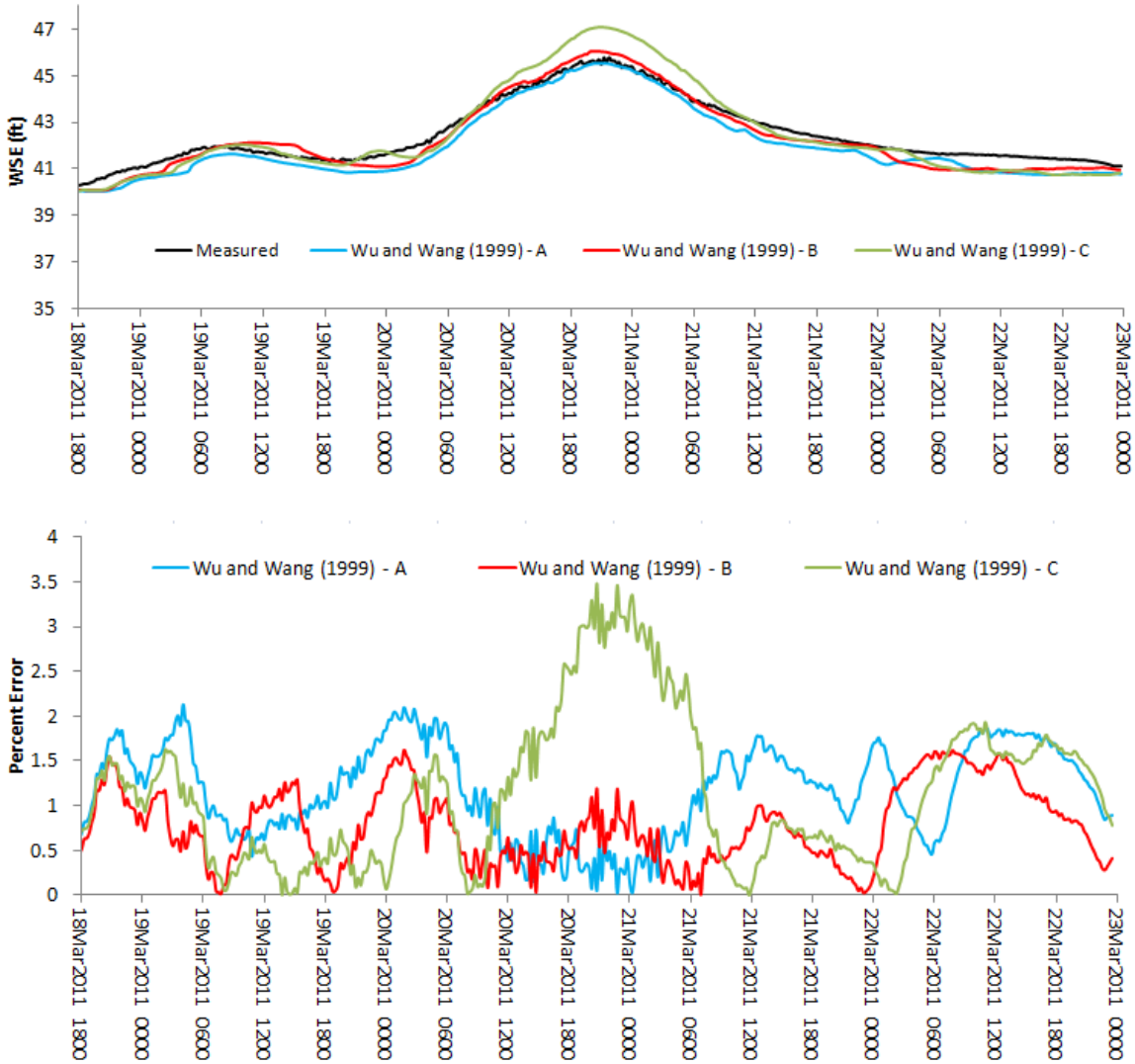


Figure 4.8 (a) Results of CCHE2D water surface elevation at Rd 102 for various grain size distributions, (b) percent error of simulated water surface elevations at Rd 102 for various grain size distributions

Table 4.2 Normalized root mean square error for simulated water surface elevations at Rd 102 for each bed roughness method

| | Wu and Wang (1999) | van Rijn (1986) | n = 0.03 |
|---|---|---|---|
| NRMSE | 0.07 | 0.13 | 0.12 |

### 4.1.2 Validation by 18-22 March 2011 flow event inside CCSB

After calibration of the roughness formula by observed water elevations at Road 102 for 18-22 March 2011 event, simulated water elevations at the overflow weir and at site C are validated by the observed counterparts.

For 18-22 March 2011 event validation inside CCSB, inlet boundary flow data was taken from instantaneous flow data at the Cache Creek at Yolo gauge (source: http://nwis.waterdata.usgs.gov, USGS 11452500) which provides 15-minute flow data. The validation simulation ran from March 18, 2011 16:45 through March 22, 2011 20:45 and had a maximum discharge of 15900 cfs (exceedance probability 41.4-percent). Simulation results are plotted in Figure 4.9 along with water surface elevation data provided by USGS (B. Brazelton, personal communication, November, 4, 2011) at Road 102, Site C in the interior of the CCSB, and at the overflow weir. The inflow boundary flow hydrograph is also provided in Figure 4.9. There is good agreement between the water surface elevation simulated by CCHE2D and the measured data provided by USGS for each of the validation points: Rd 102, site C, and the overflow weir. The locations of these validation points are referenced in Figure 4.4. The performance of the numerical model can be represented by the NRMSE, as described in the previous section, as well as by the Nash-Sutcliffe Model Efficiency coefficient (Nash Coefficient). The Nash Coefficient is a means of assessing the predictive power of hydrological models and is defined as $E = 1 - \frac{\sum_{t=1}^{T}(Q_0^t - Q_m^t)^2}{\sum_{t=1}^{T}(Q_0^t - \overline{Q_0})^2}$, where $Q_0$ are the observed field values, and $Q_m$ are the simulated model values. An efficiency of 1 (E = 1) corresponds to a perfect match between model values and the observed values. The NRMSE and Nash Coefficient for both validation cases, and the validation simulation are presented in Table 4.3.

Table 4.3 NRMSE and Nash Coefficient for calibration and validation simulations

| Event | 18-22 March 2011 | | | 23-27 March 2011 | | |
|---|---|---|---|---|---|---|
| Peak Flow at Cache Creek at Yolo | 15,900 cfs | | | 14,300 cfs | | |
| Mode | Calibration | Validation | | Validation | | |
| Location | Rd 102 | Site C | Weir | Rd 102 | Site C | Weir |
| NRMSE | 0.07 | 0.11 | 0.09 | 0.12 | 0.07 | 0.08 |
| Nash Coefficient | 0.93 | 0.83 | 0.90 | 0.69 | 0.90 | 0.87 |

The inflow hydrograph shown in Figure 4.9 also indicates four specific time steps for which water depth and velocity contour plots are provided in later figures. Water depth and velocity magnitude results from the calibration simulation for the extent of Cache Creek between Yolo and Rd 102 at time steps 1 through 4 are presented in Figures 4.10-4.13. Note that the units displayed are metric corresponding to the computational format of CCHE2D. Water depth and velocity magnitude results from the validation simulation for the CCSB are presented in Figures 4.14-4.17. Water depth contours indicate inundation area of the basin, and are shown for select time references, as indicated in Figure 4.9. Velocity magnitudes are displayed in Figures 4.16 and 4.17 for those select time references. Velocity magnitude and vectors indicating direction of flow for the southern portion of the settling basin, including the terminus of the training

channel, low flow channel, and overflow weir are provided in Figures 4.18 through 4.21 for the four time steps indicated. Velocity vectors are scaled relative to each other. However, magnitudes must be read from the contour provided.

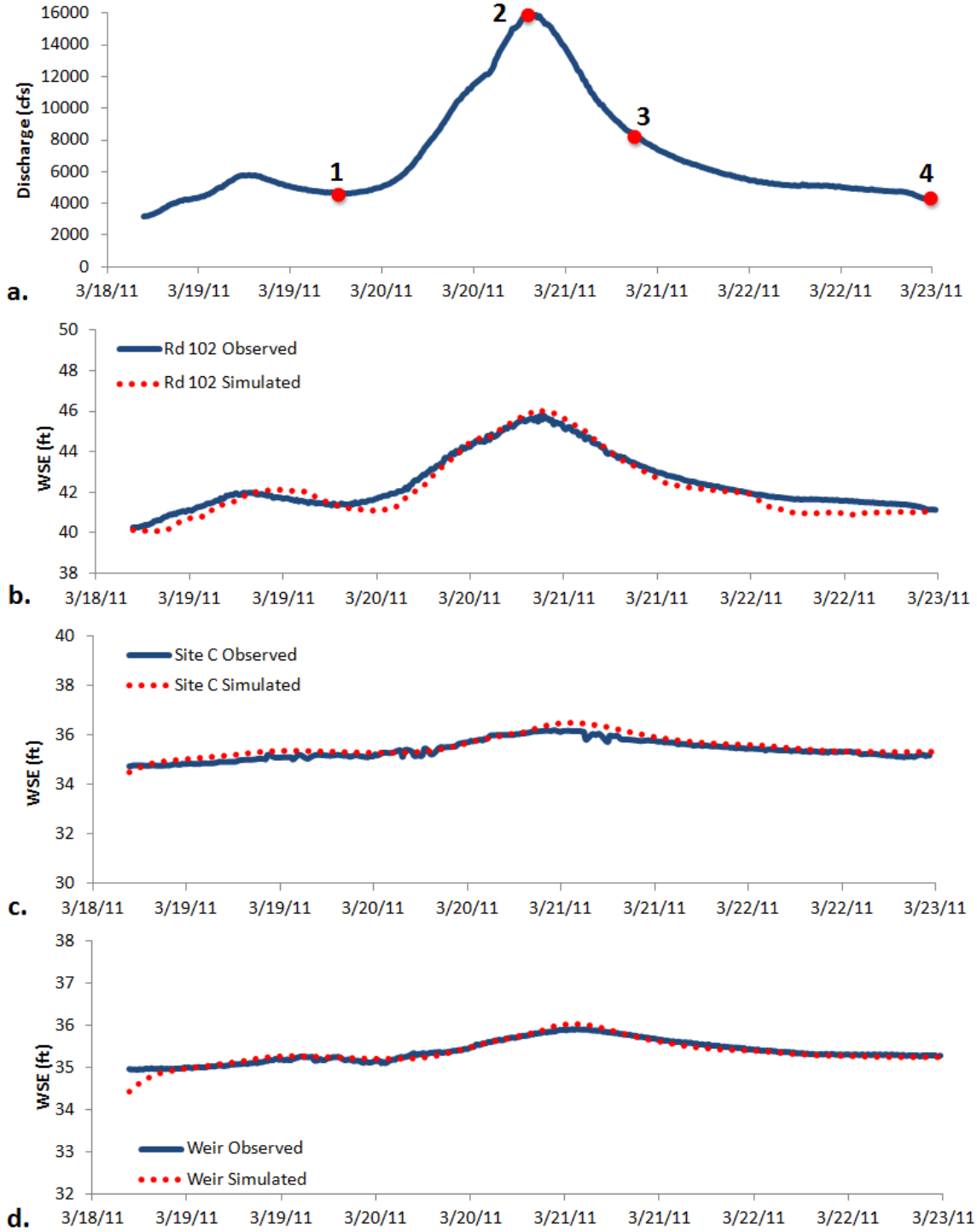


Figure 4.9 Comparison plots of 18-22 March 2011 simulation, (a) Inflow discharge at Cache Creek at Yolo with time steps for results display, (b) Calibrated water surface elevation at Rd 102 for entire simulation duration, (c) Water Surface Elevation validation at Site C for entire simulation duration, (d) Water Surface Elevation validation at Overflow Weir for entire simulation duration

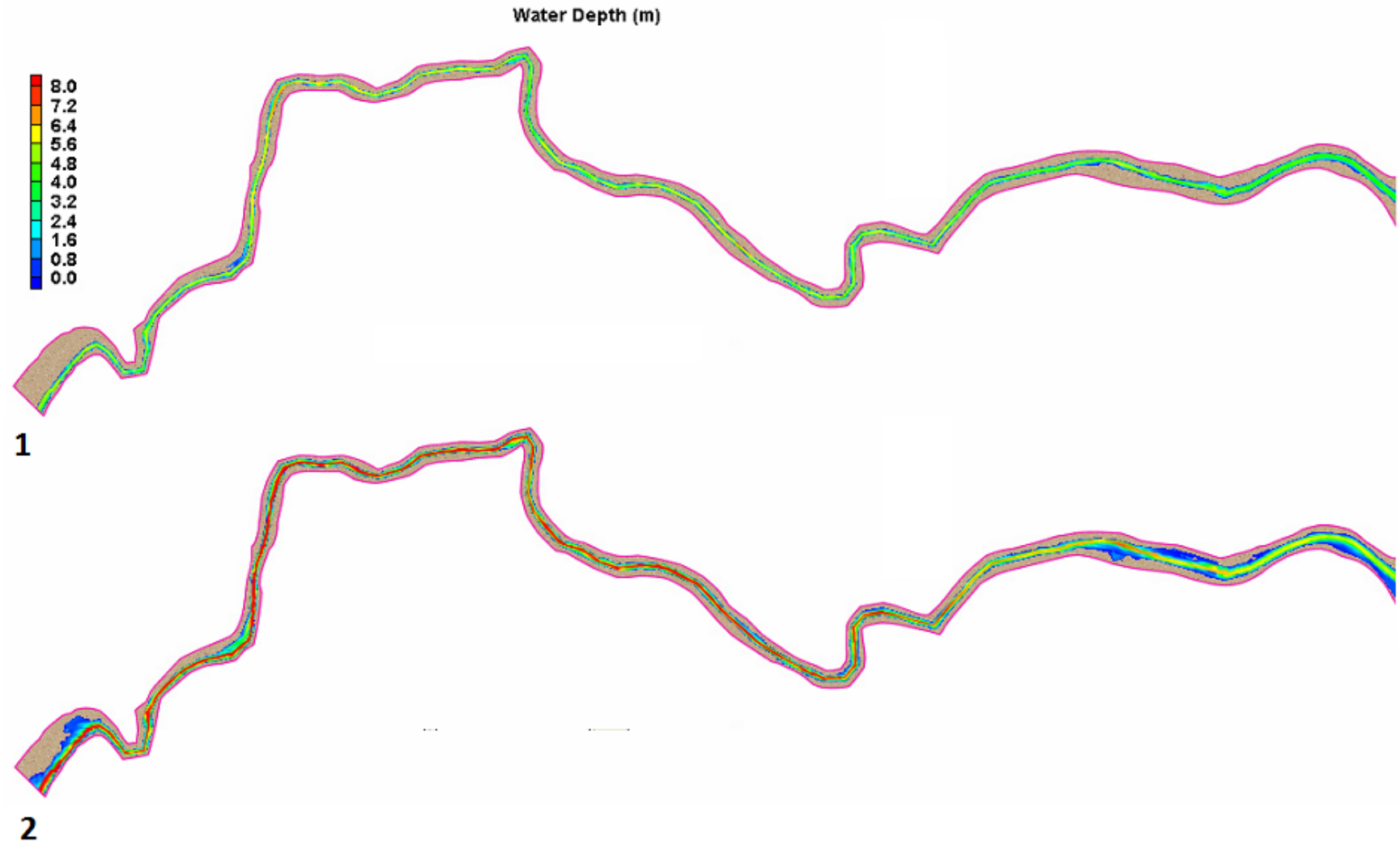


Figure 4.10 Water depth results at selected times on rising limb of storm hydrograph, 1 and 2 (peak flow) of 18-22 March 2011 event; Cache Creek at Yolo to Rd 102

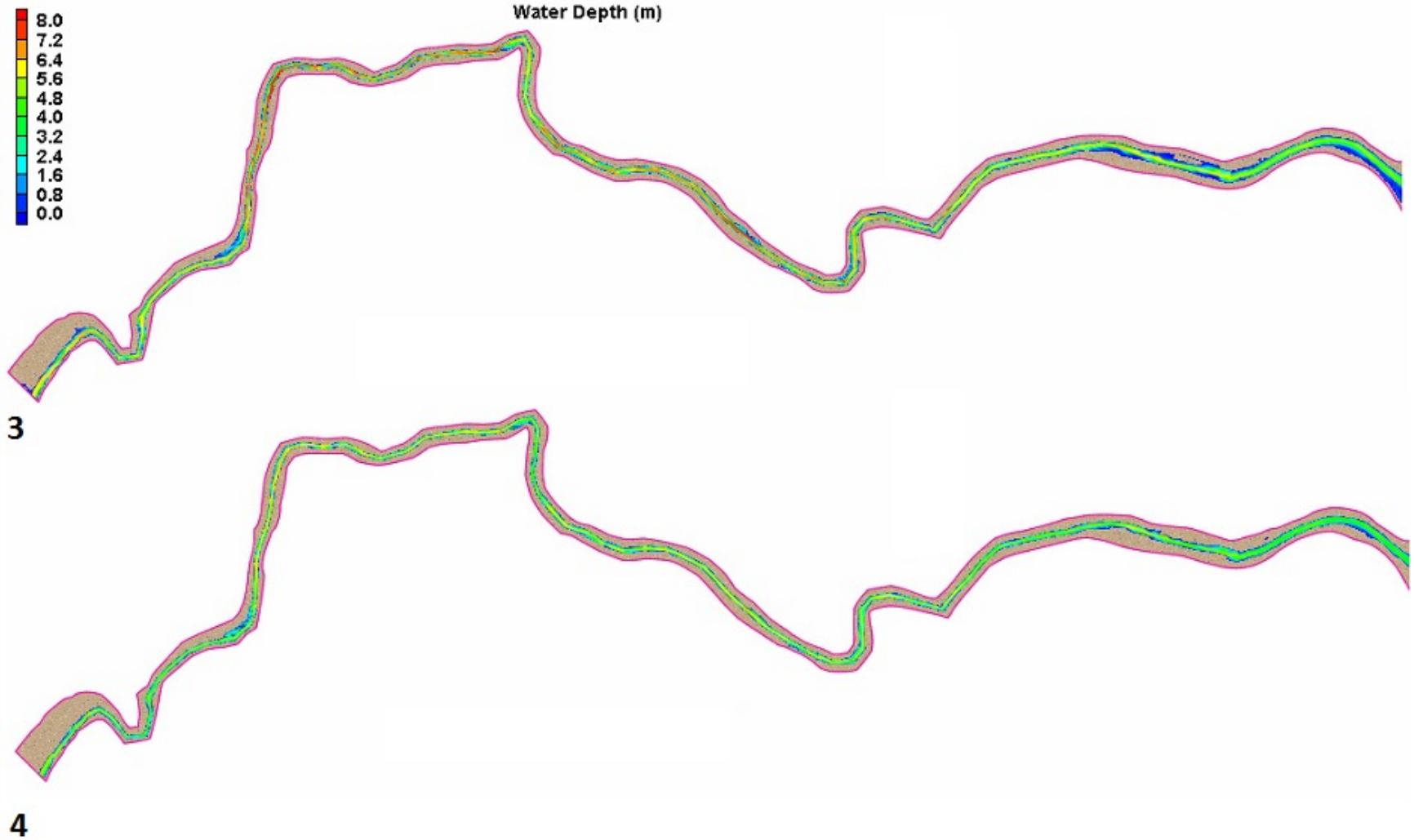


Figure 4.11 Water depth results at selected times on falling limb of hydrograph, 3 and 4 of 18-22 March 2011 event; Cache Creek at Yolo to Rd 102

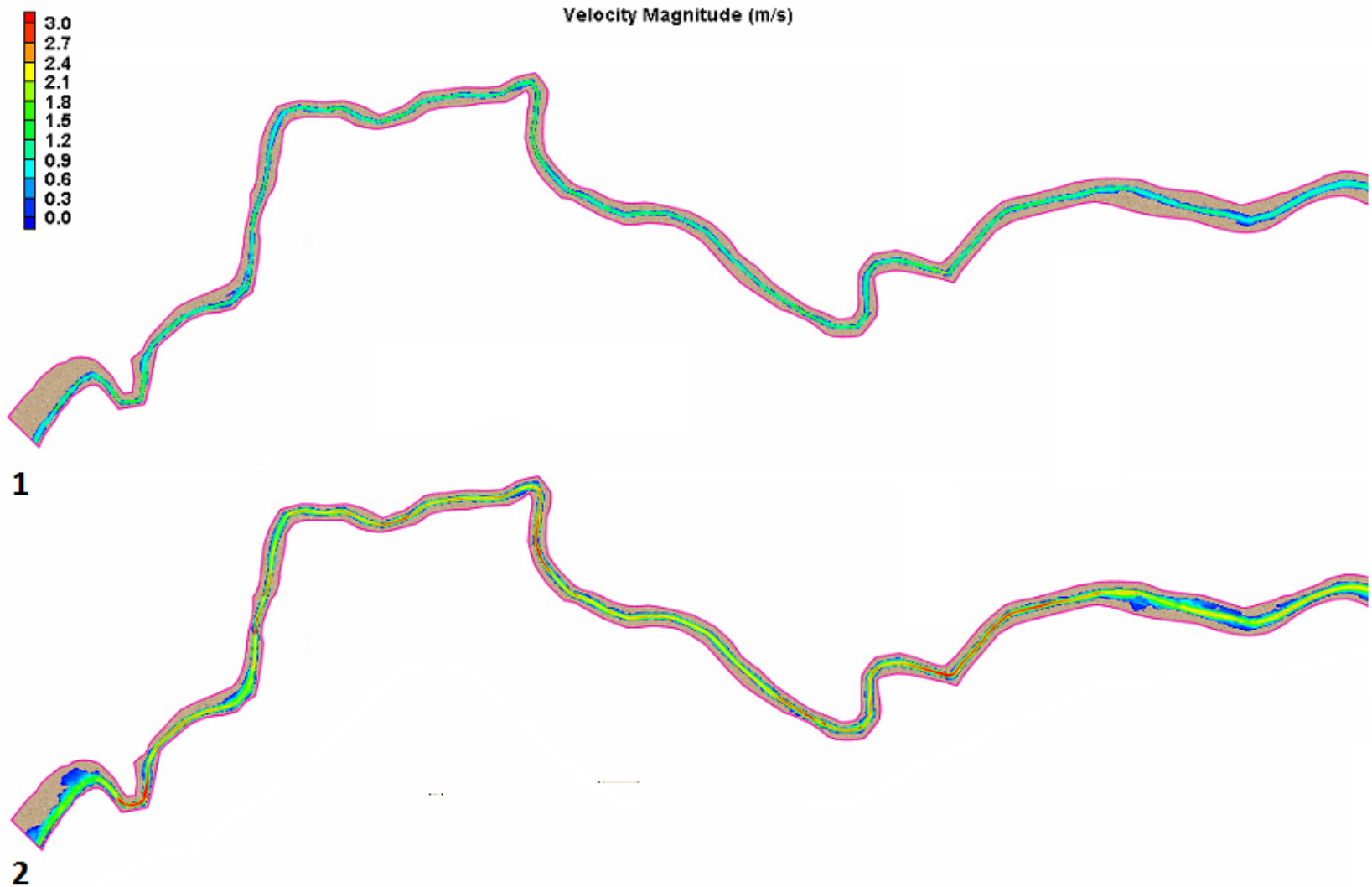


Figure 4.12 Velocity magnitude results at selected times on rising limb of hydrograph, 1 and 2 (peak flow) of 18-22 March 2011 event; Cache Creek at Yolo to Rd 102

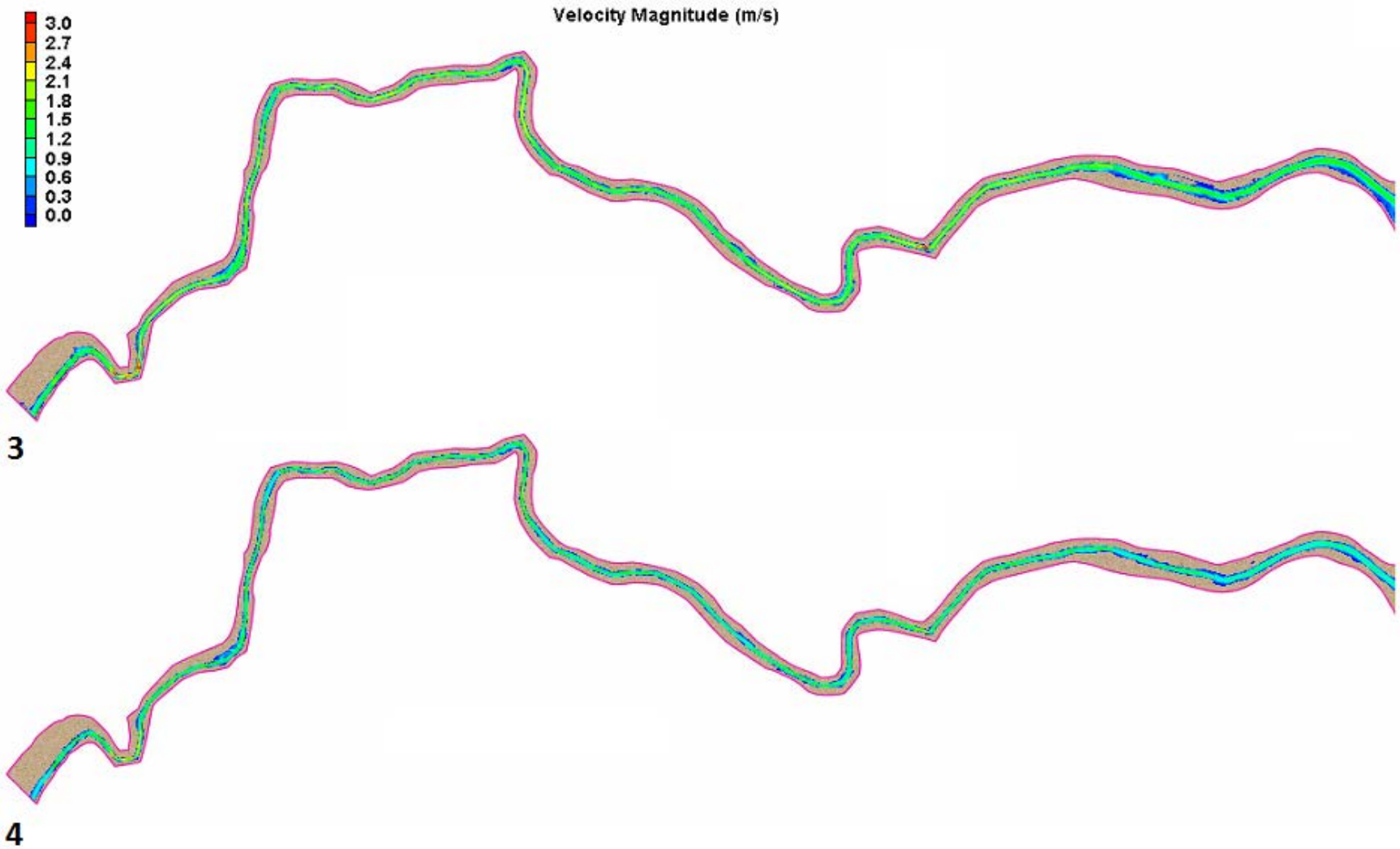


Figure 4.13 Velocity magnitude results at selected times on falling limb of hydrograph, 3 and 4 of 18-22 March 2011 event; Cache Creek at Yolo to Rd 102

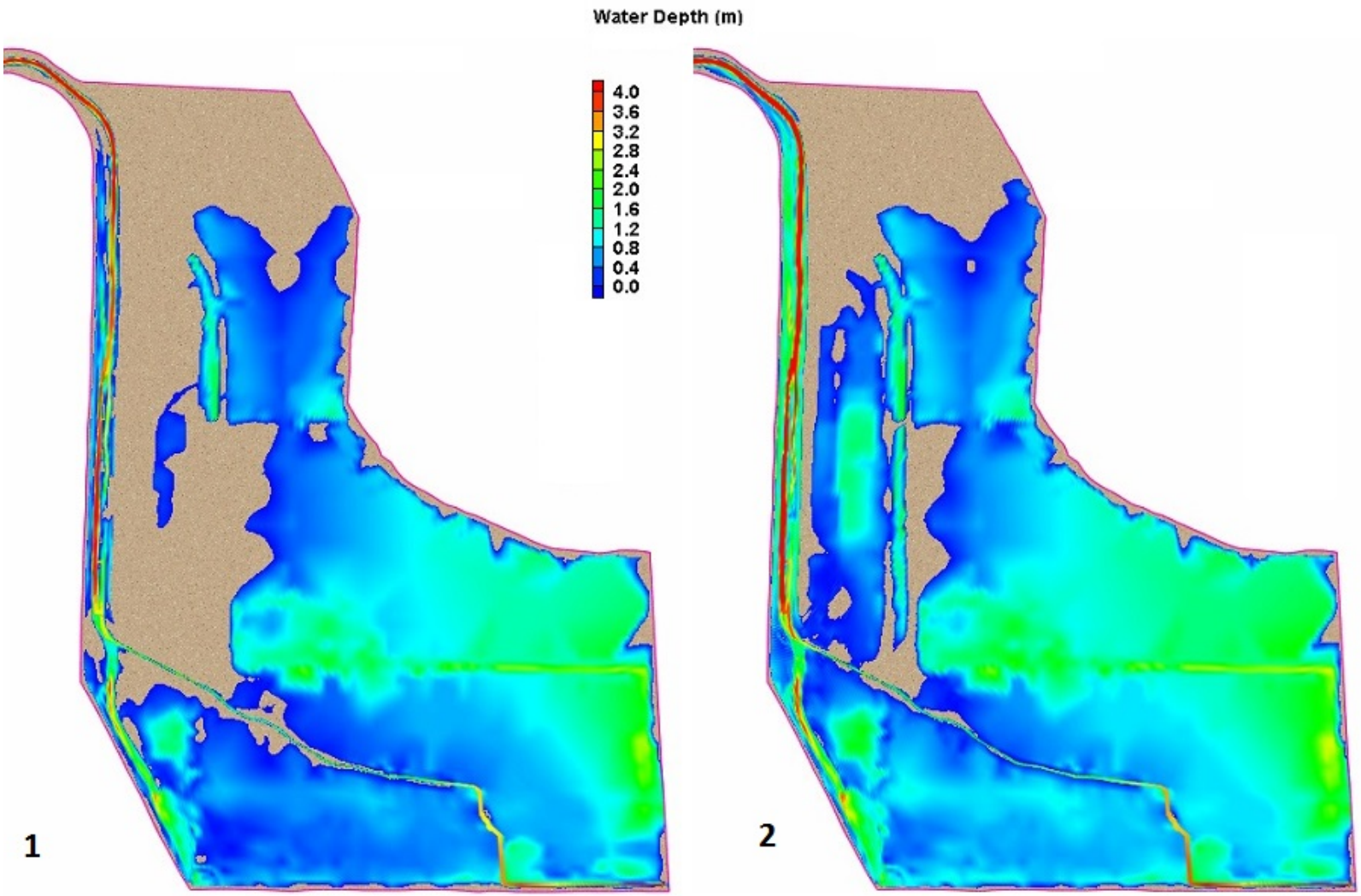


Figure 4.14 CCSB water depth results, March 2011, at selected times on rising limb of hydrograph, 1 and 2 (peak flow) of 18-22 March 2011 event.

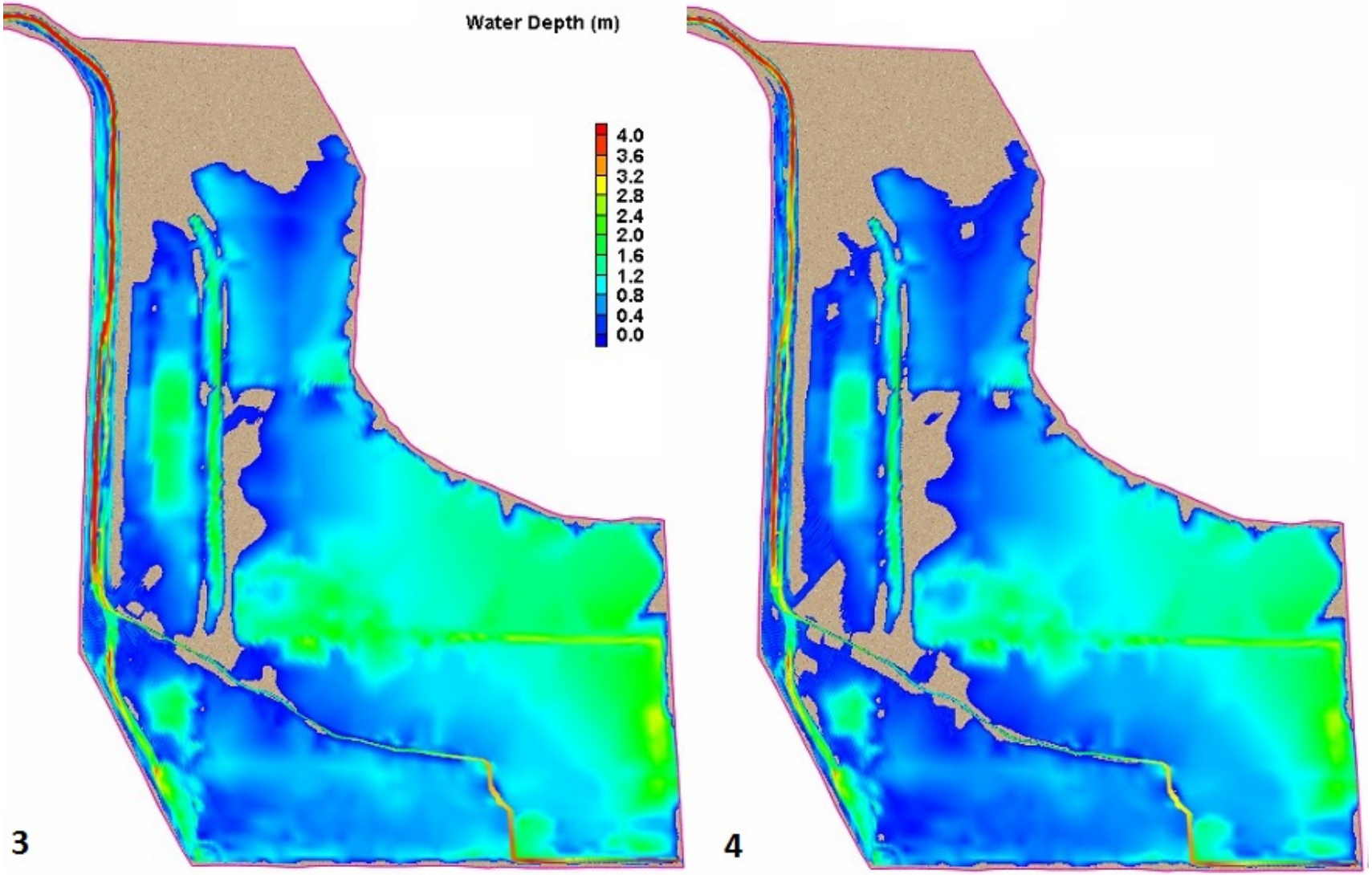


Figure 4.15 CCSB water depth results, March 2011, at selected times on falling limb of hydrograph, 3 and 4 of 18-22 March 2011 event

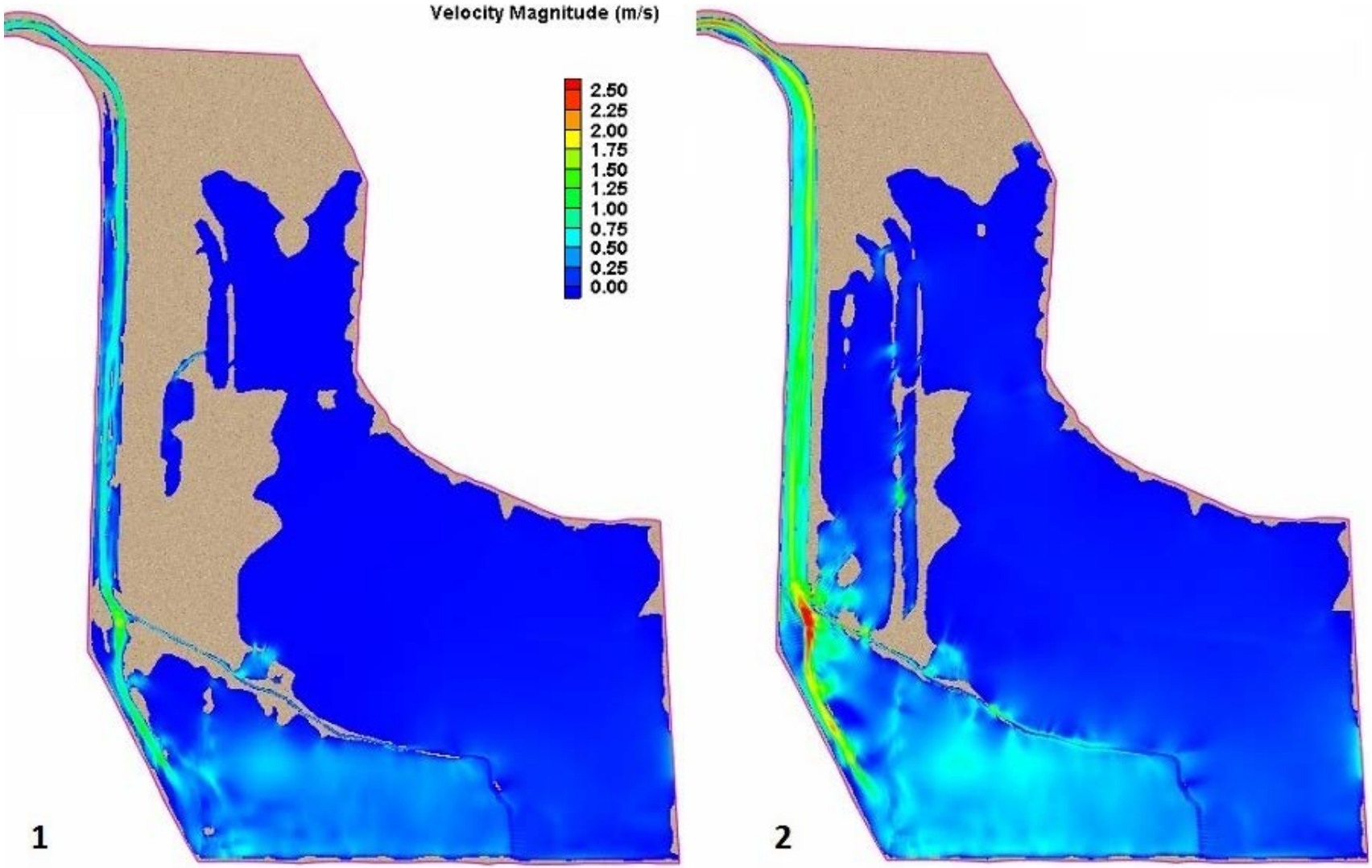


Figure 4.16 CCSB velocity magnitude results, March 2011, at selected times on rising limb of hydrograph, 1 and 2 (peak flow) of 18-22 March 2011 event

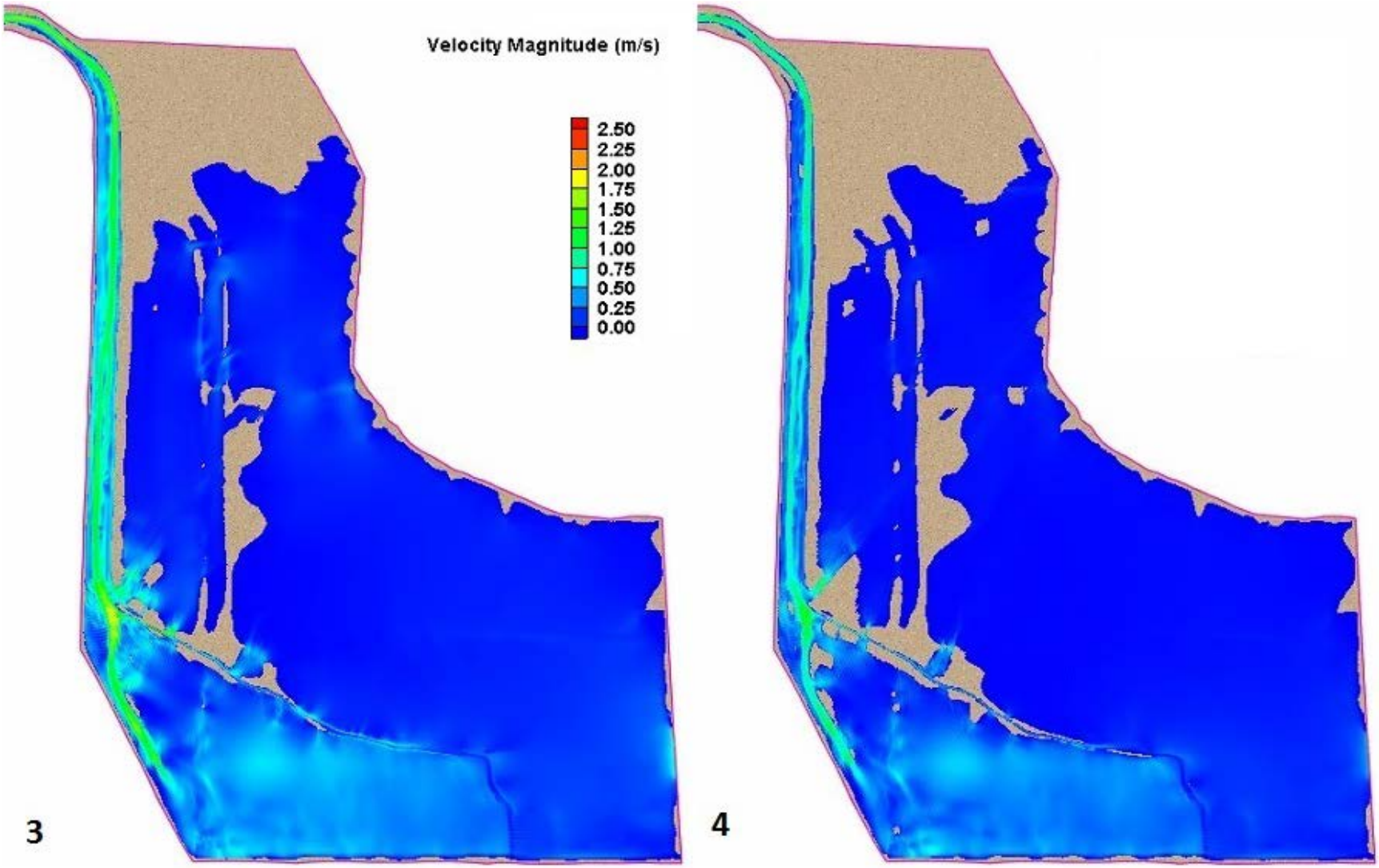


Figure 4.17 CCSB velocity magnitude results, March 2011, at selected times on falling limb of hydrograph, 3 and 4 of 18-22 March 2011 event

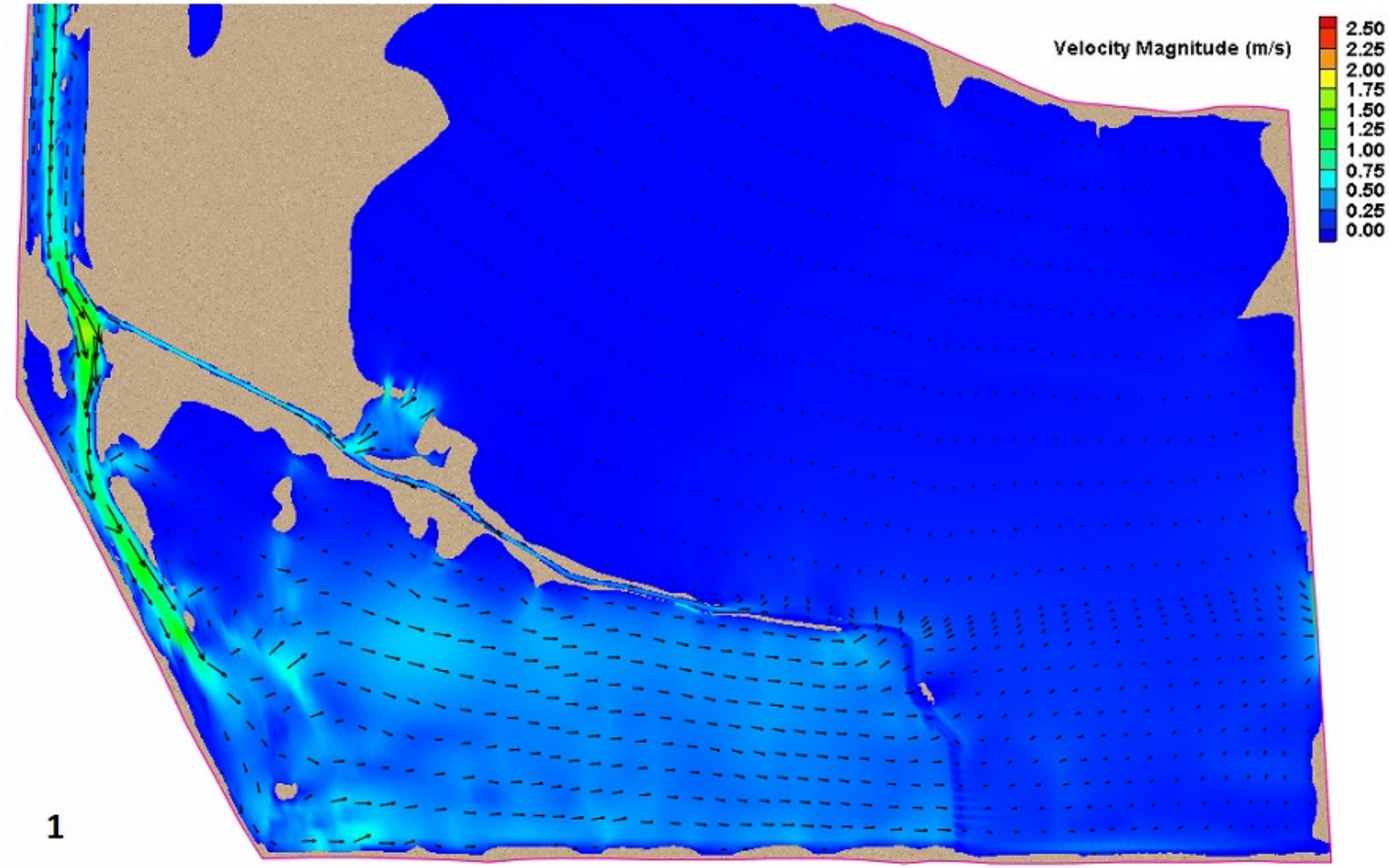


Figure 4.18 CCSB velocity magnitude result with scaled directional vectors, at selected time 1 of 18-22 March 2011 event

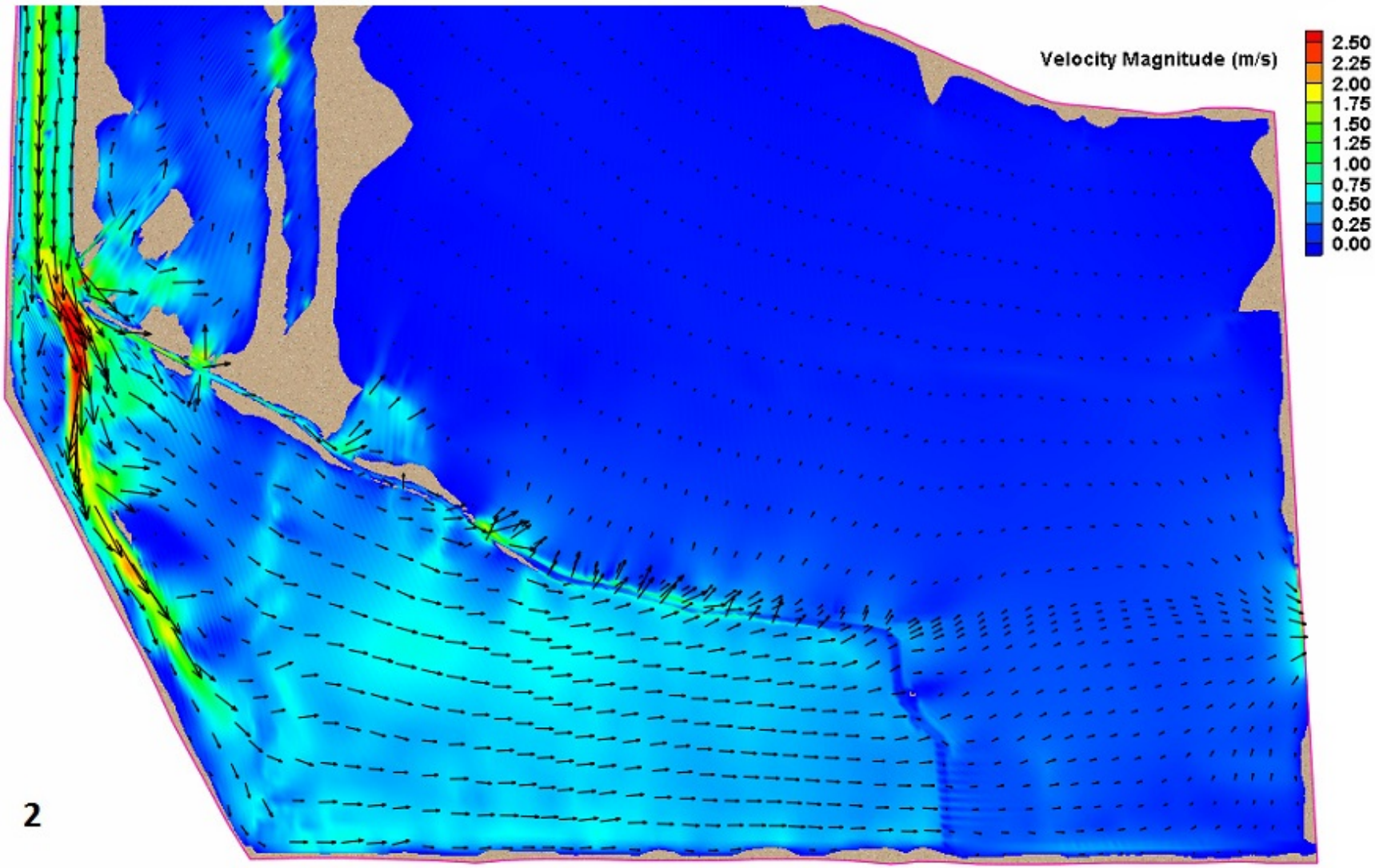


Figure 4.19 CCSB velocity magnitude result with scaled directional vectors, at selected time 2 of 18-22 March 2011 event

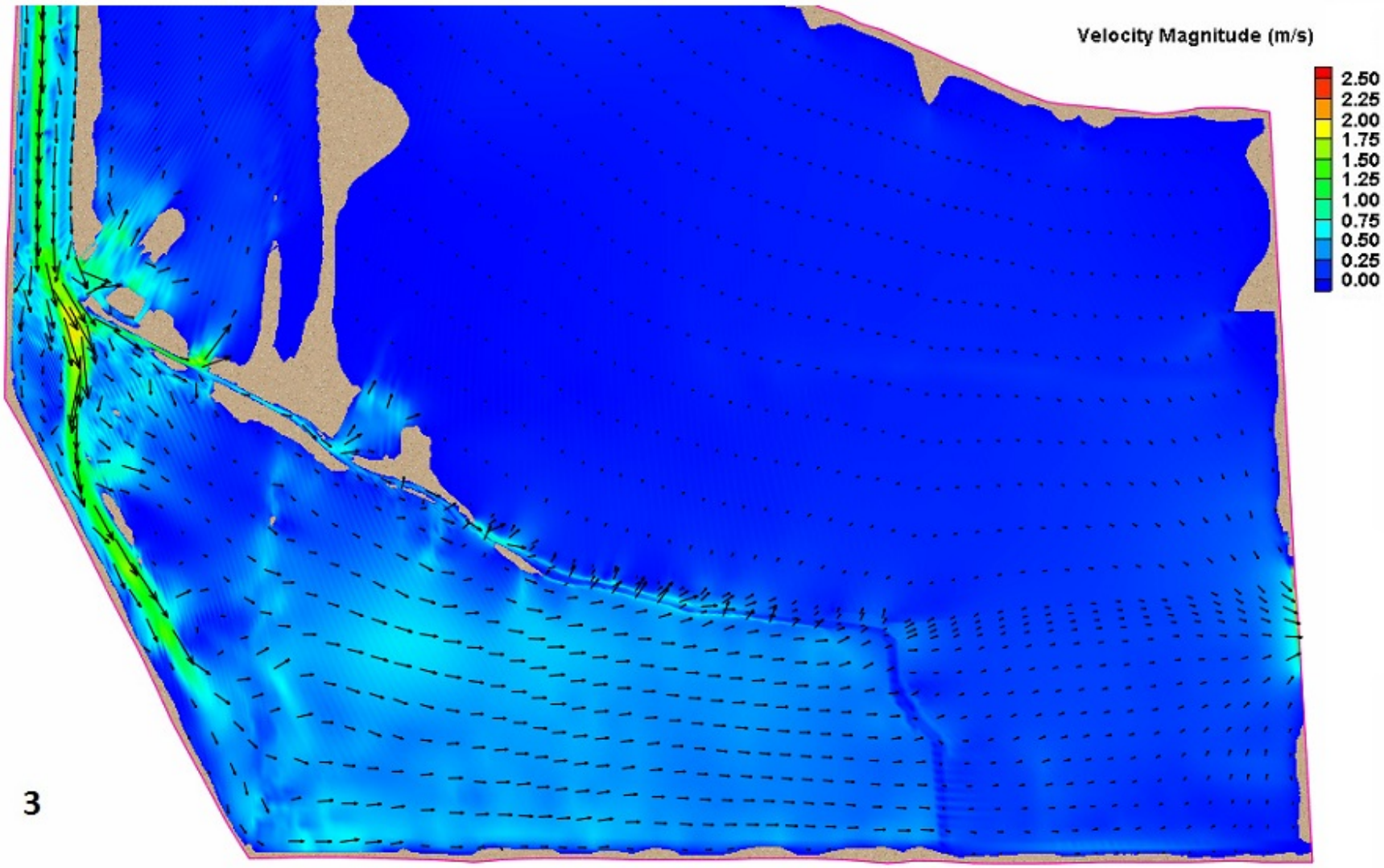


Figure 4.20 CCSB velocity magnitude result with scaled directional vectors, at selected time 3 of 18-22 March 2011 event

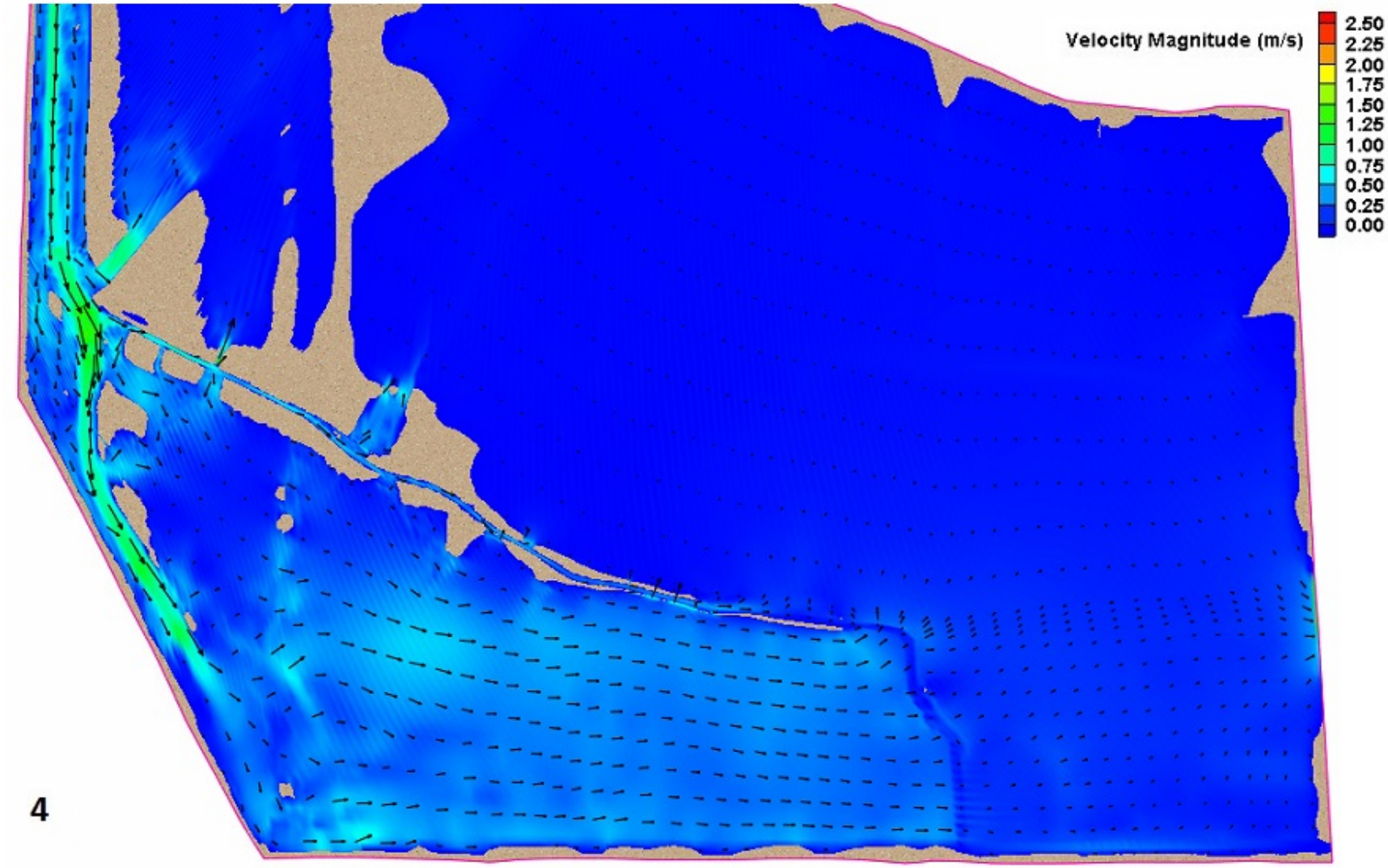


Figure 4.21 CCSB velocity magnitude result with scaled directional vectors, at selected time 4 of 18-22 March 2011 event

### 4.1.3 Validation by 23-27 March 2011 flow event at Road 102 and inside CCSB

A validation simulation was conducted for the full extent of the simulation mesh shown in Figures 3.20 and 3.21 and for an inflow boundary condition for flow set as discharge at Yolo from March 23, 2011 04:15 through March 27, 2011 23:45, with a peak flow discharge of 14,300 cfs, a flow with an exceedance probability of 50-percent. The inflow hydrograph presented in Figure 4.22, is a storm hydrograph with multiple peaks, the largest of which occurs near the mid-point of the nearly 5-day hydrograph duration (labeled time selection 3). The simulation results are plotted, along with water surface elevation data collected during the storm event at Rd 102, Site C and the Overflow Weir in Figure 4.22. There is good agreement between modeled and measured water surface elevation data, illustrating that the model is capable of simulating transient flows, and can handle wetting and drying of the CCSB as inundation area directly relates to water surface elevation. Table 4.3 contains the NRMSE and Nash Coefficient results for the validation simulation. At site C and the overflow weir the NRMSE is less 0.05 or less, and the Nash Coefficient is greater than 0.87, demonstrating that the model is predicting inundation and water surface elevation very well. Water surface elevations at the weir are in good agreement throughout the simulation, suggesting that discharge is also well represented through the duration. Water surface elevation contours for select times in the storm hydrograph are shown in Figure 4.23 through 4.25 for the extent from Yolo to Rd 102, and in Figure 4.26 through 4.28 for the CCSB from Rd 102 to the outlets. Velocity contours at select time steps, for the extent from Yolo to Rd 102, are shown in Figures 4.29 through 4.31. The velocity contours for the CCSB are shown in Figures 4.32 through 4.34. Figures 4.35 through 4.39 contain velocity contours and velocity vectors for the southern portion of the CCSB, focusing on the terminus of the training levee, the low flow channel and the overflow weir. Velocity vectors are scaled relative to each other. However, the magnitudes must be read from the contours.

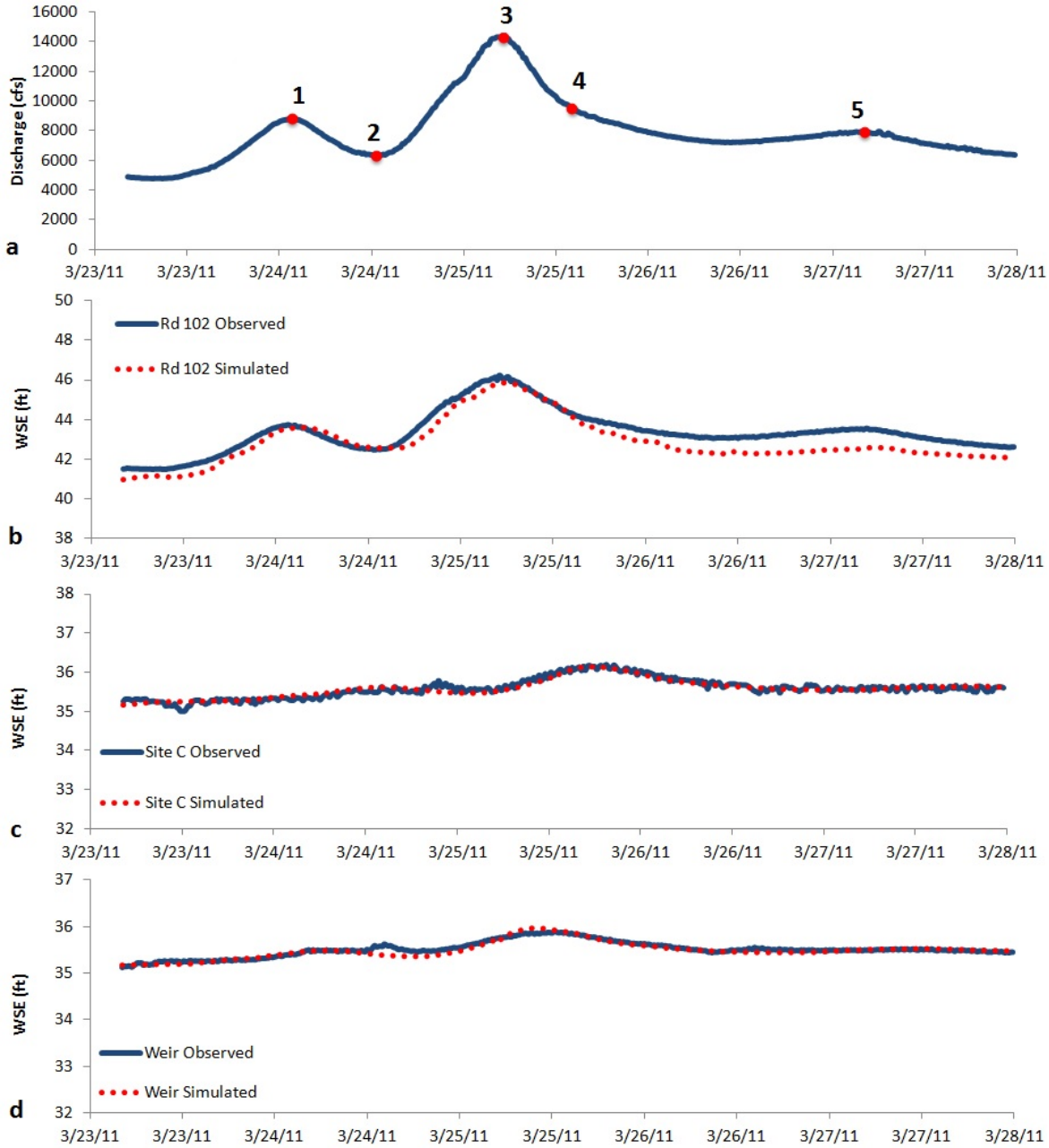


Figure 4.22 Comparison plots of 23-27 March 2011 validation simulation, (a) Inflow discharge at Cache Creek at Yolo with time steps for results display, (b) Water surface elevation validation at Rd 102 for entire simulation duration, (c) Water Surface Elevation validation at Site C for entire simulation duration, (d) Water Surface Elevation validation at Overflow Weir for entire simulation duration

Figure 4.23 Water depth validation simulation results, Yolo to Rd 102, at selected times 1 and 2 of 23-27 March 2011 event

Figure 4.24 Water depth validation simulation results, Yolo to Rd 102, at selected times 3 (peak flow) and 4 of 23-27 March 2011 event

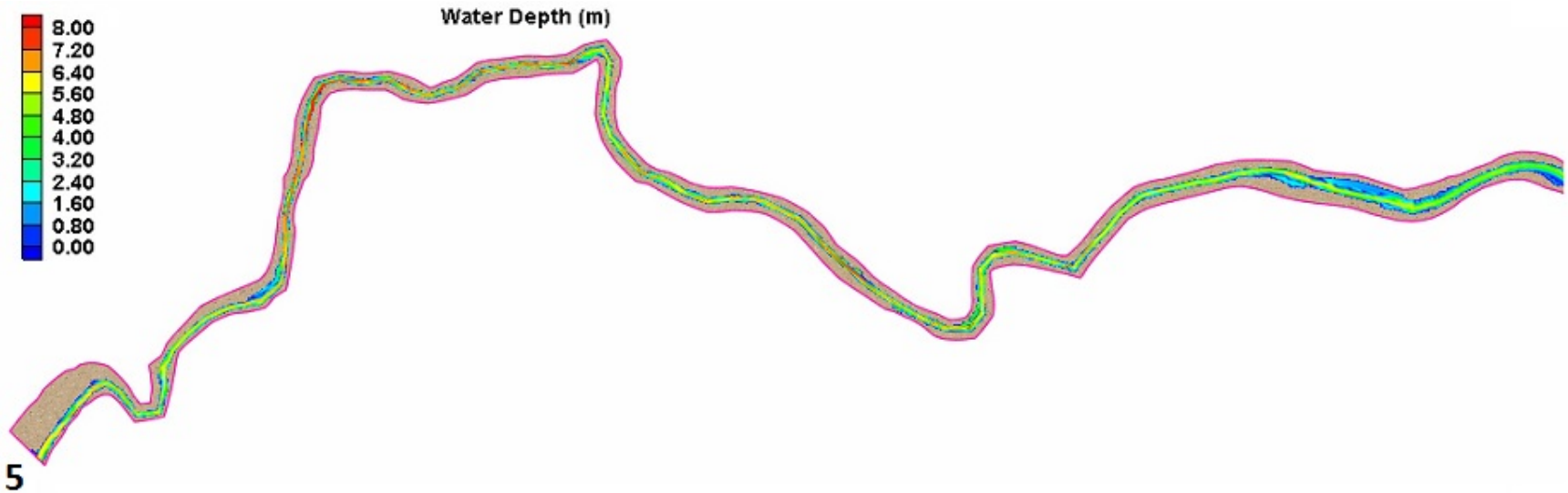

Figure 4.25 Water depth validation simulation results, Yolo to Rd 102, at selected time 5 of 23-27 March 2011 event

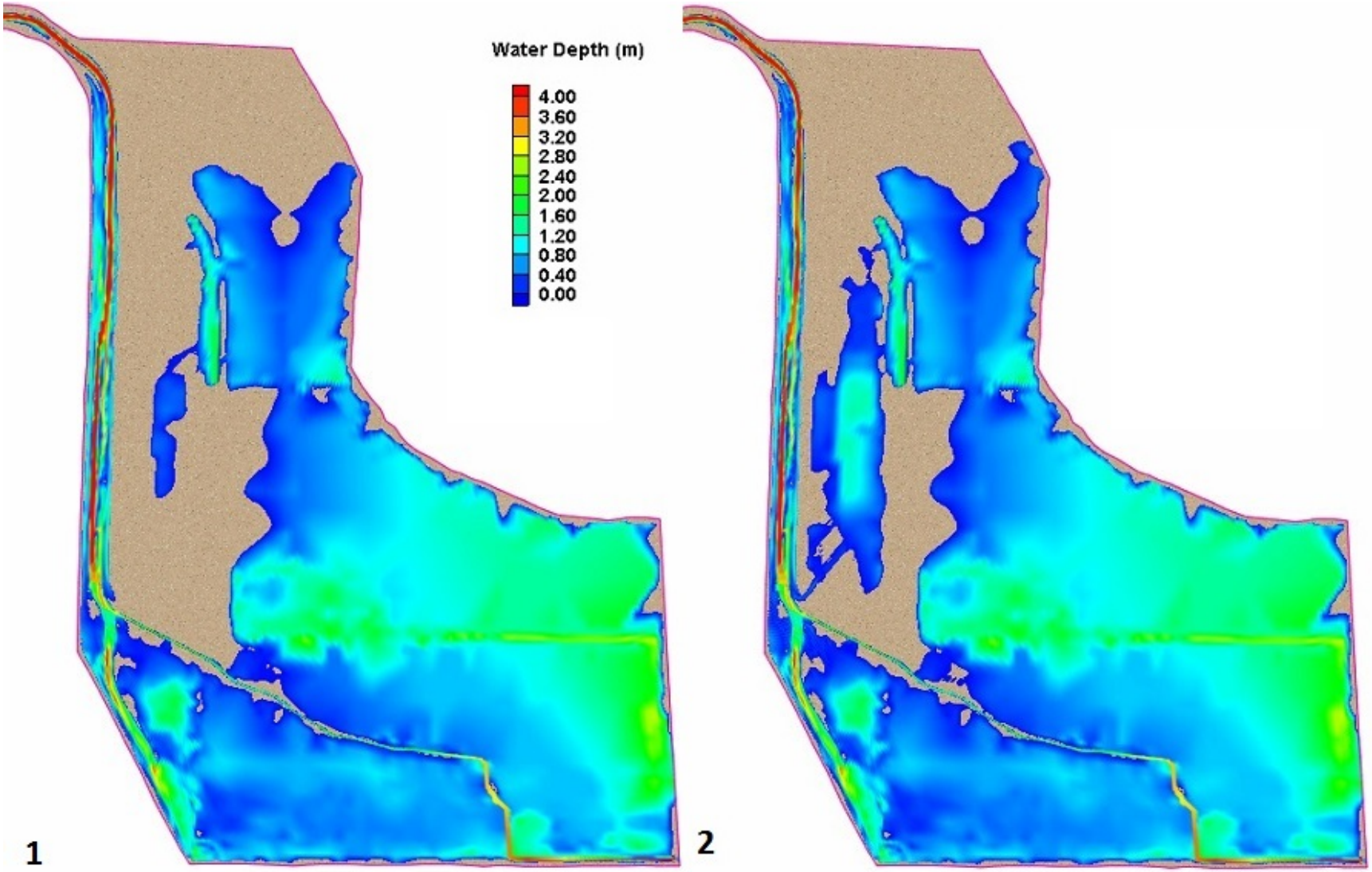


Figure 4.26 Water depth validation results, CCSB, at selected times 1 and 2 of 23-27 March 2011 event

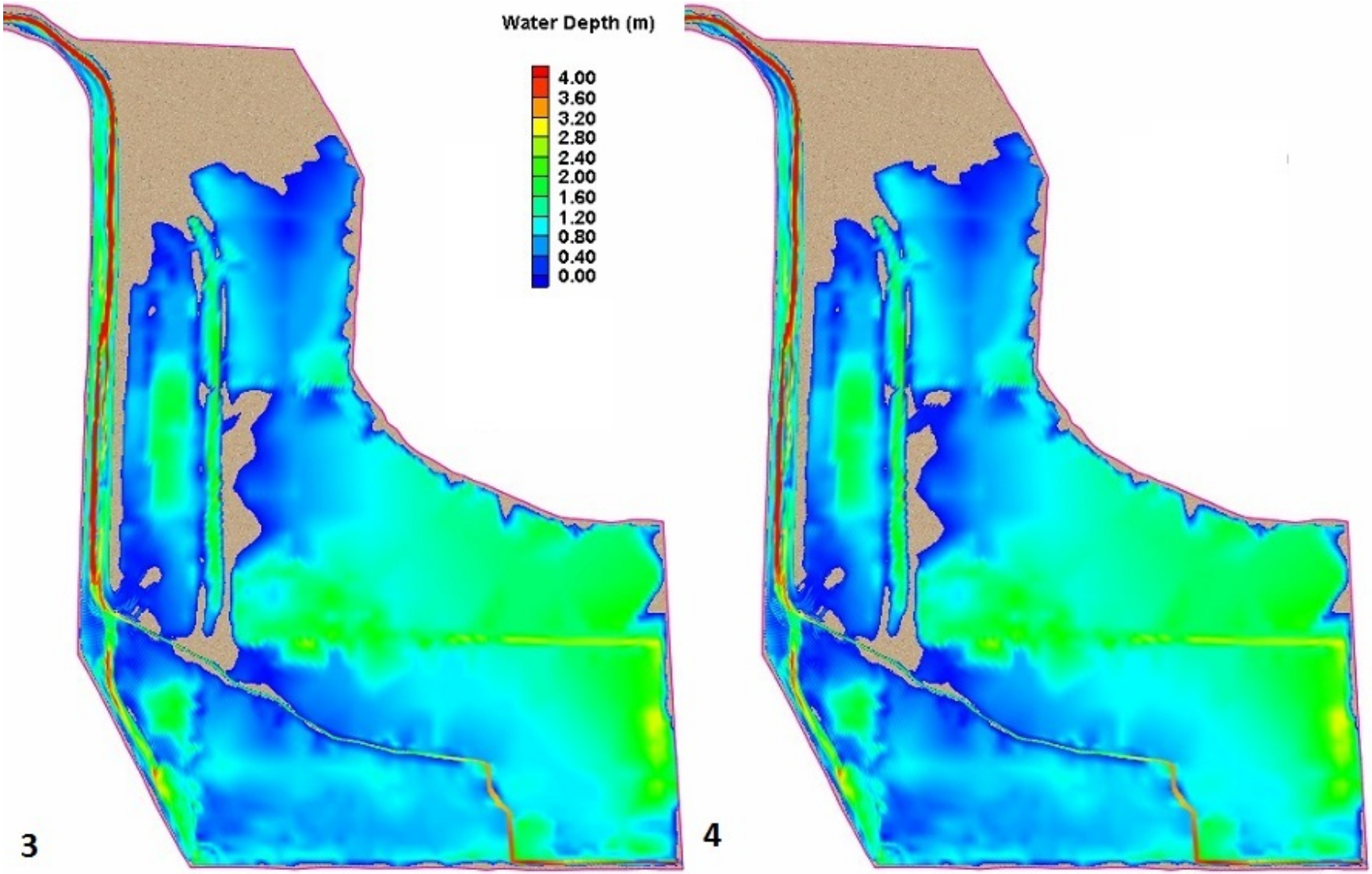


Figure 4.27 Water depth validation results, CCSB, at selected times 3 (peak flow) and 4 of 23-27 March 2011 event

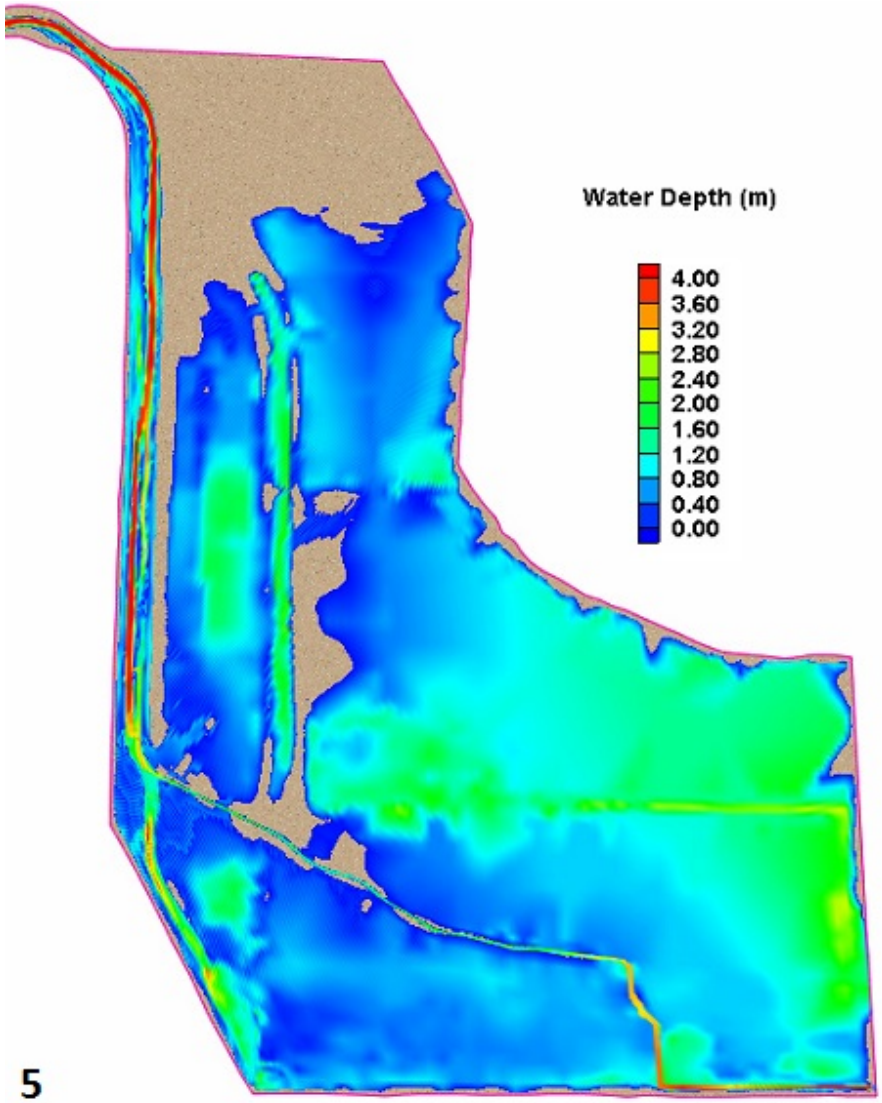

Figure 4.28 Water depth validation results, CCSB, at selected time 5 of 23-27 March 2011 event

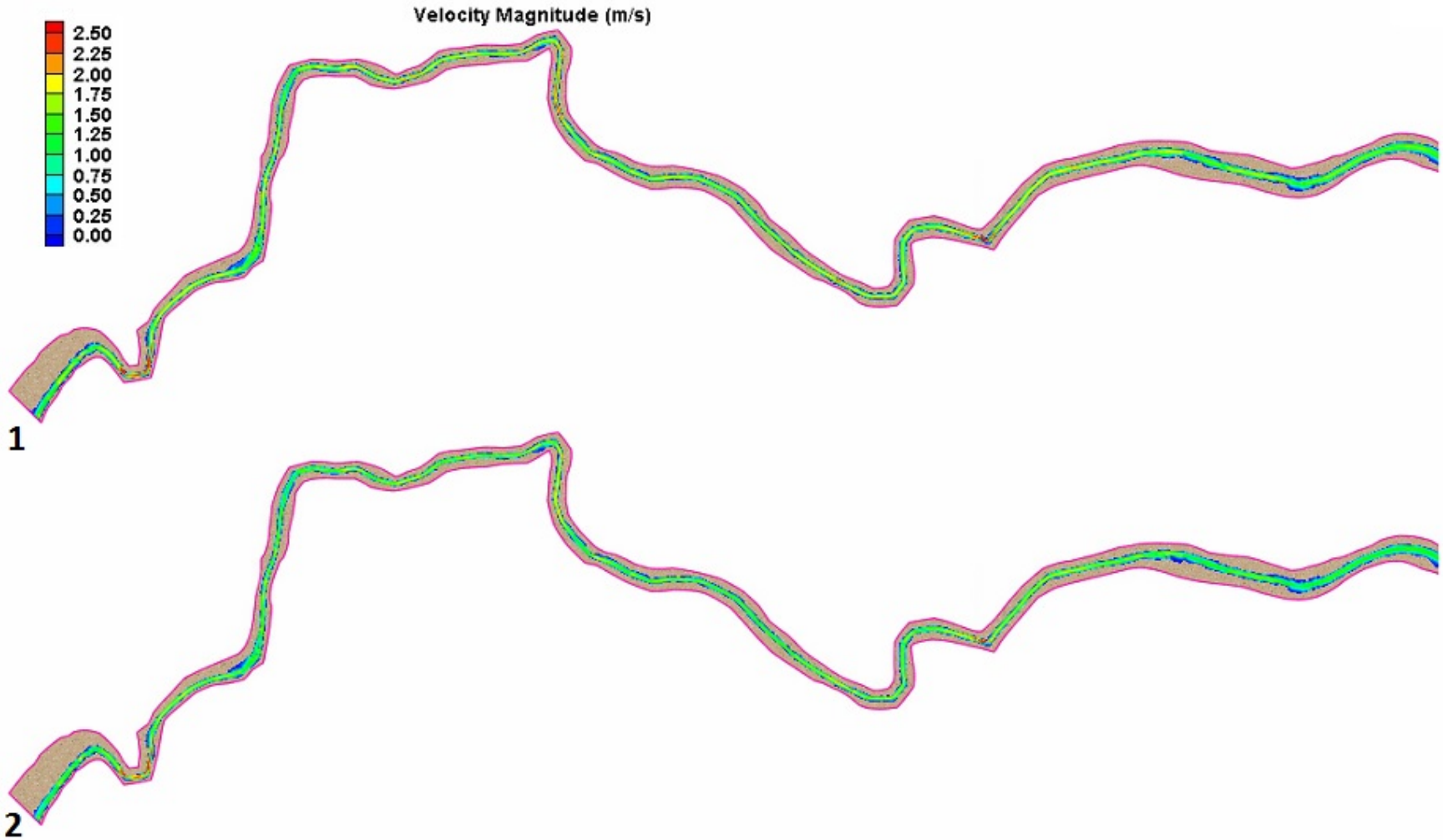

Figure 4.29 Velocity magnitude validation results, Yolo to Rd 102, at selected times 1 and 2 of 23-27 March 2011 event

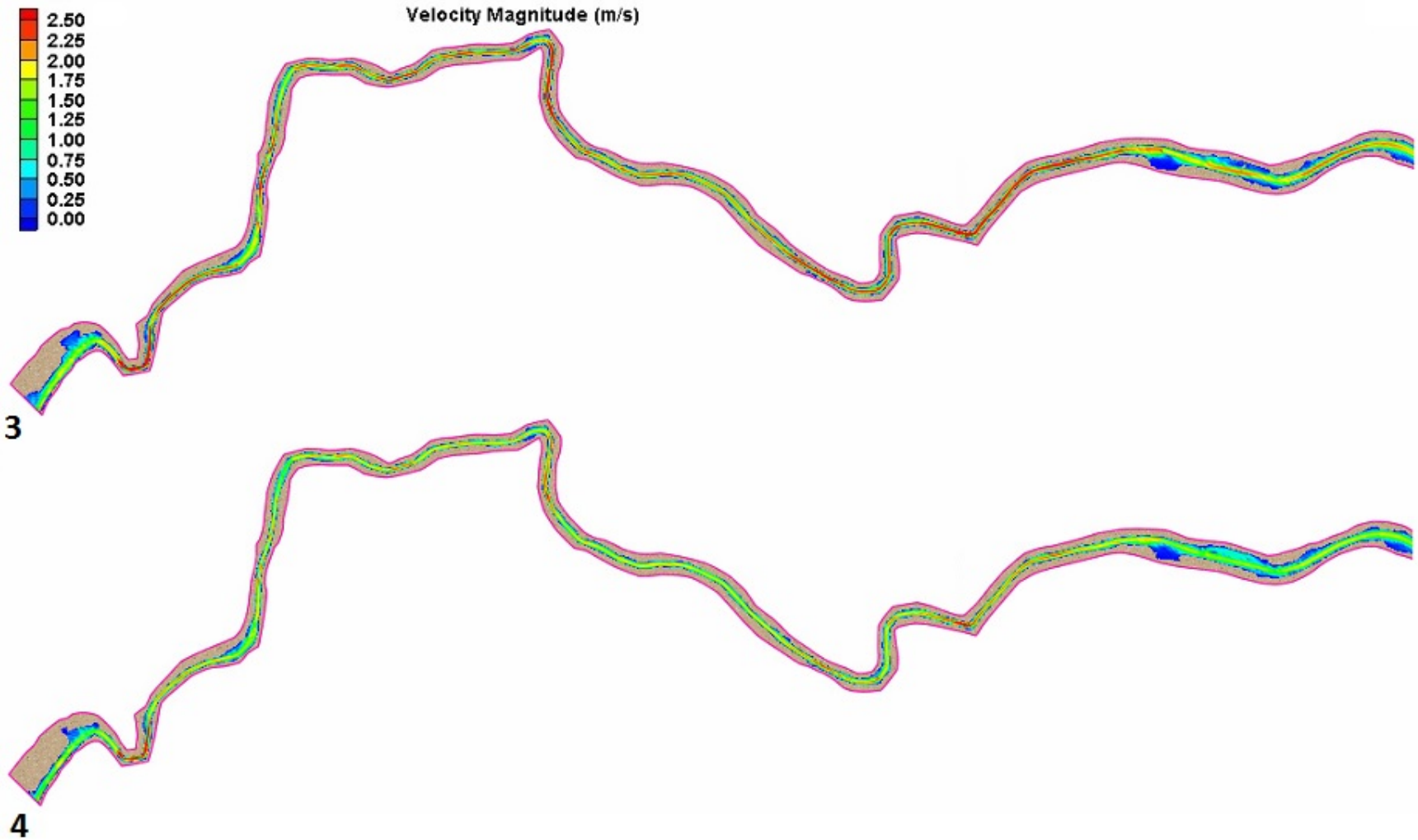

Figure 4.30 Velocity magnitude validation results, Yolo to Rd 102, at selected times 3 (peak flow) and 4 of 23-27 March 2011 event

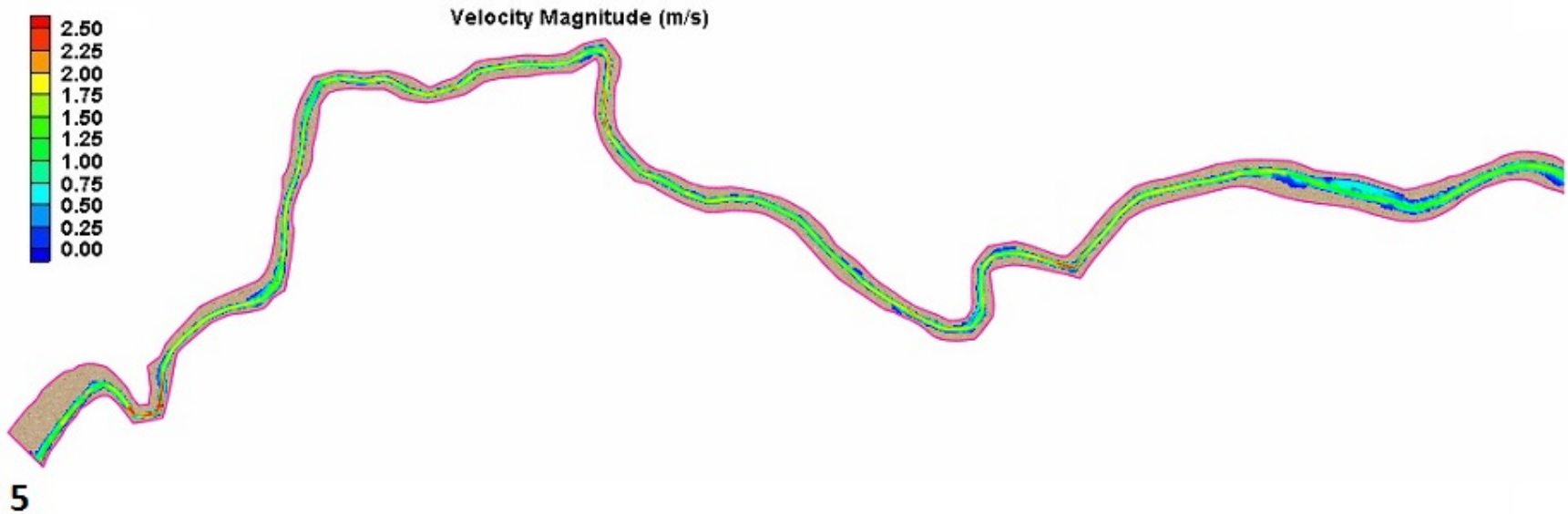

Figure 4.31 Velocity magnitude validation results, Yolo to Rd 102, at selected time 5 of 23-27 March 2011 event.

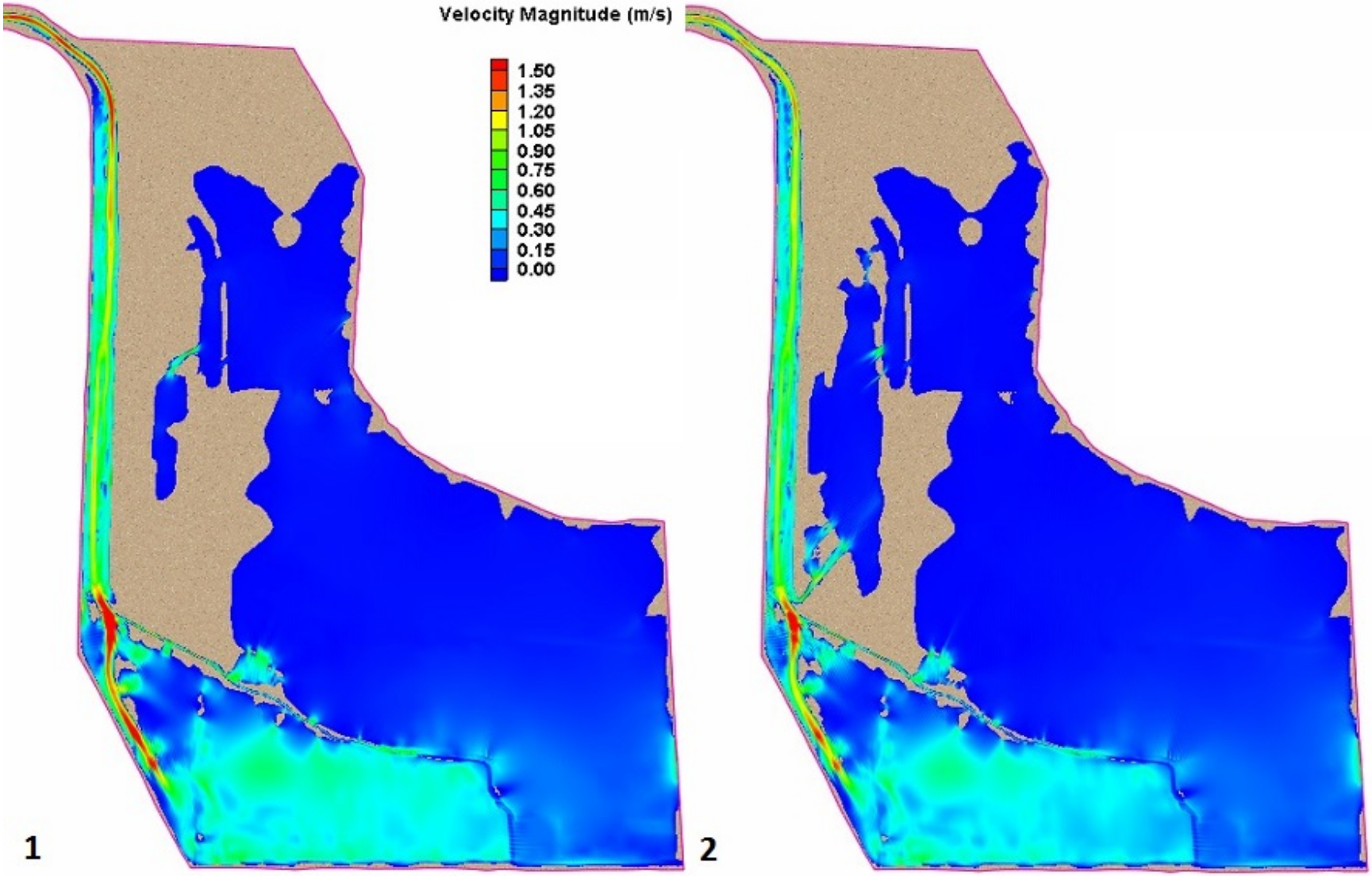


Figure 4.32 Velocity magnitude validation simulation results, CCSB, at selected times 1 and 2 of 23-27 March 2011 event

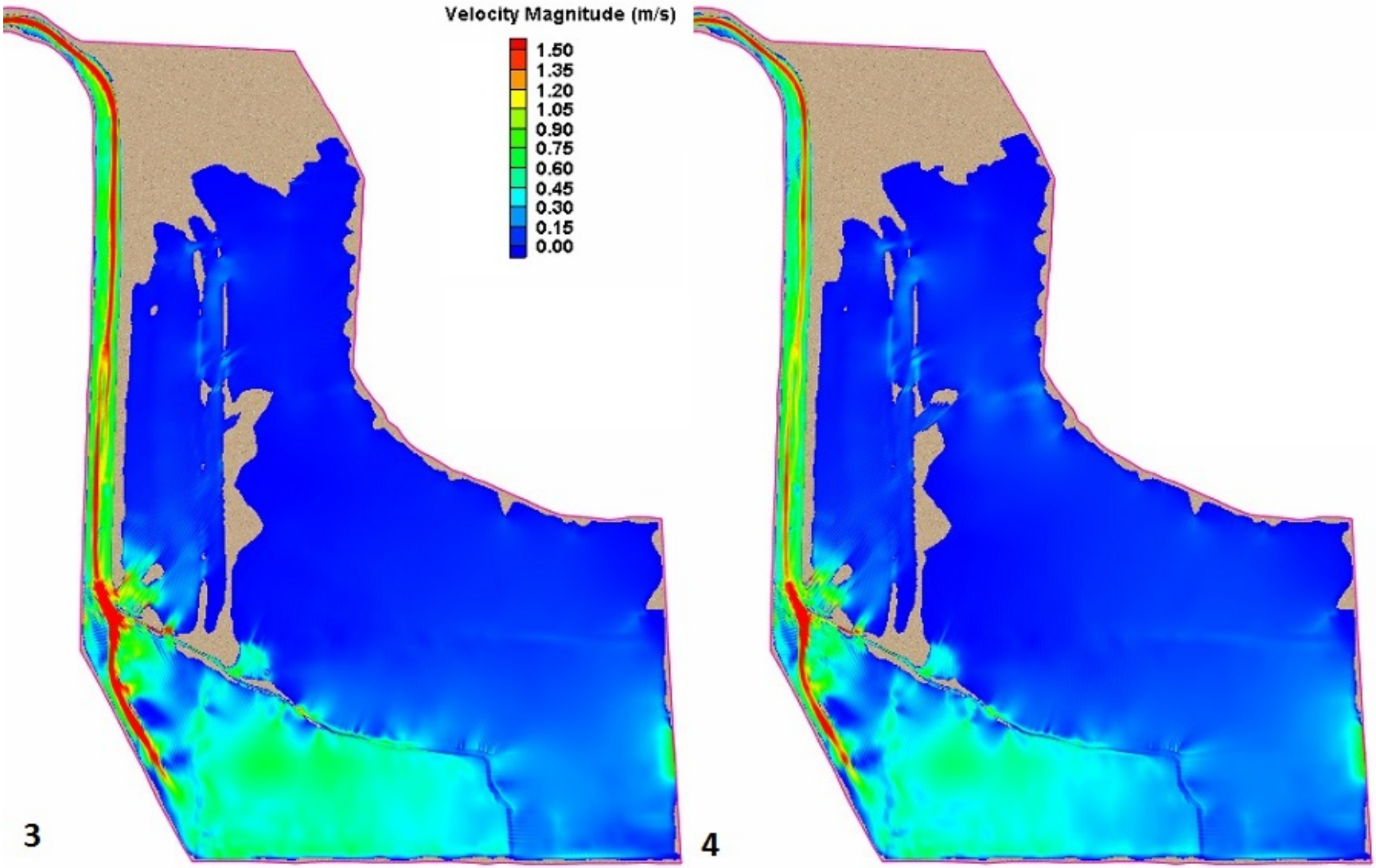


Figure 4.33 Velocity magnitude validation simulation results, CCSB, at selected times 3 (peak flow) and 4 of 23-27 March 2011 event

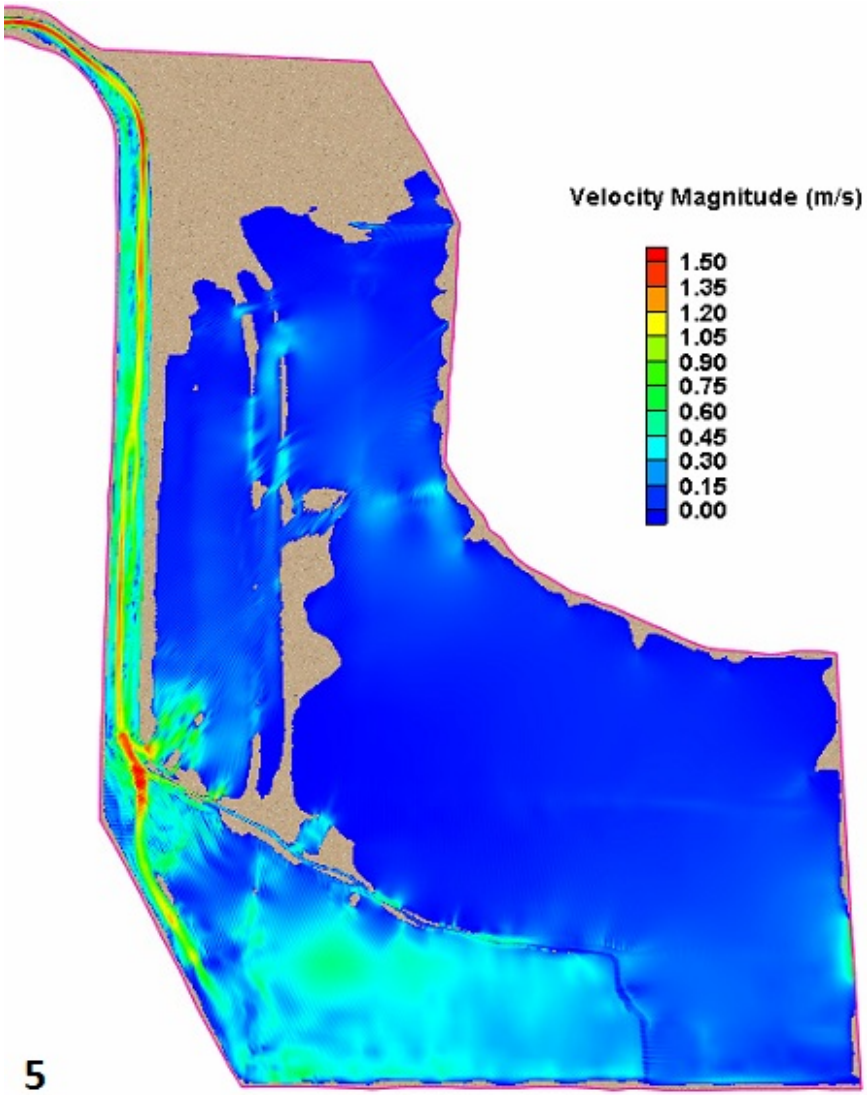

Figure 4.34 Velocity magnitude validation simulation results, CCSB, at selected time 5 of 23-27 March 2011 event

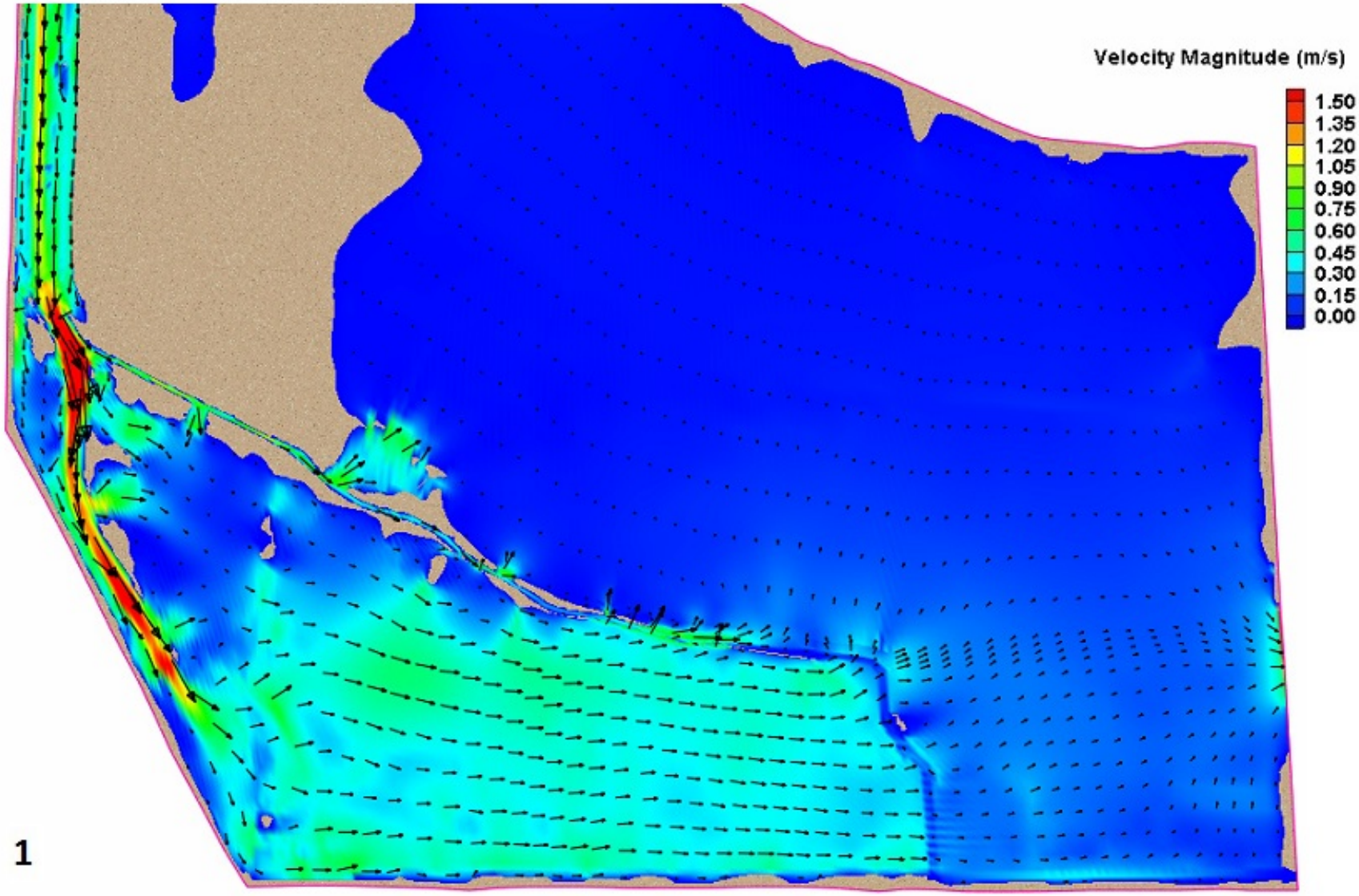
Velocity Magnitude (m/s)
1.50
1.35
1.20
1.05
0.90
0.75
0.60
0.45
0.30
0.15
0.00
1

Figure 4.35 CCSB validation velocity magnitude result with scaled directional vectors, at selected time 1 of 23-27 March 2011 event

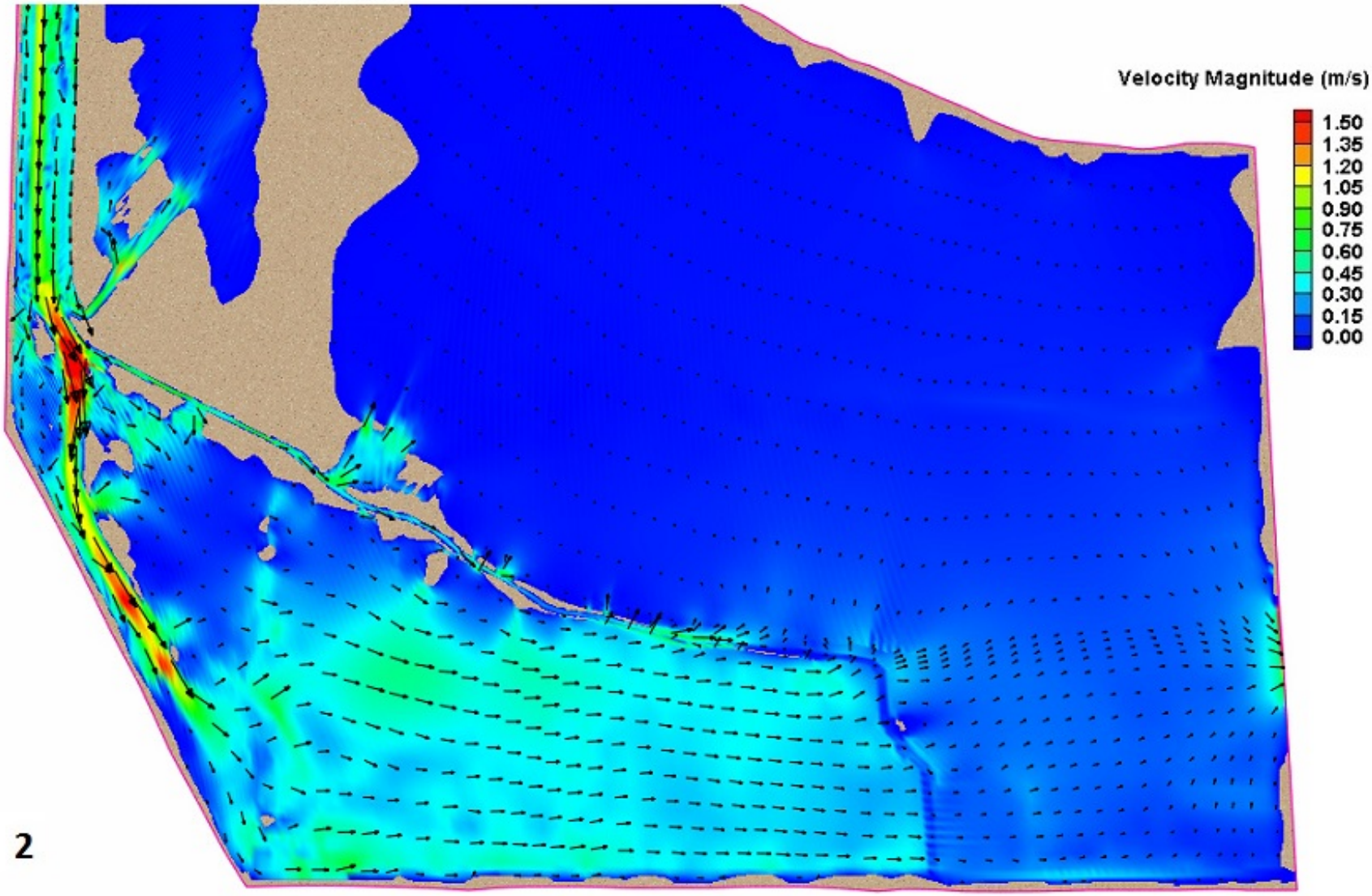


Figure 4.36 CCSB validation velocity magnitude result with scaled directional vectors, at selected time 2 of 23-27 March 2011 event

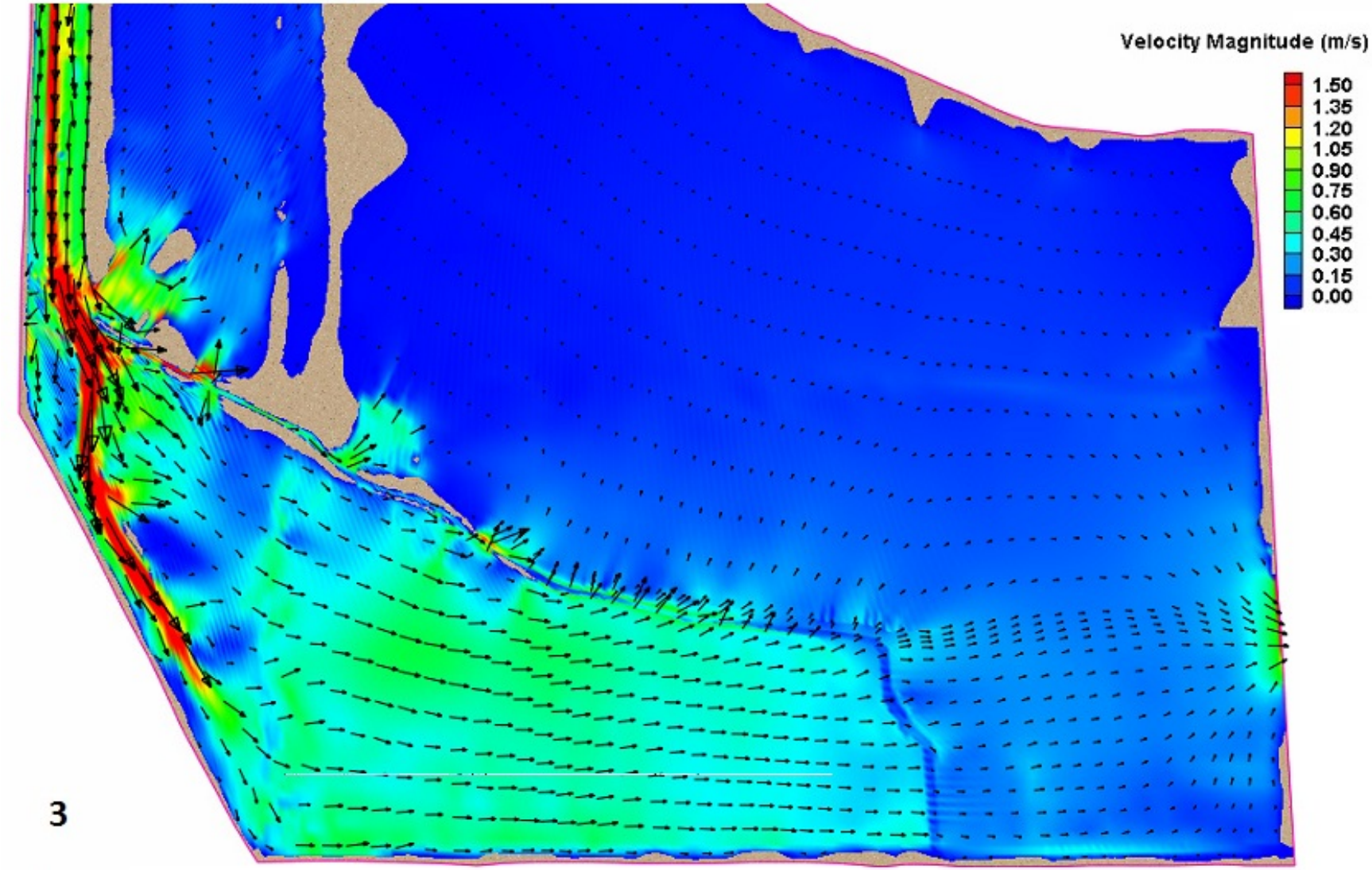


Figure 4.37 CCSB validation velocity magnitude result with scaled directional vectors, at selected time 3 (peak flow) of 23-27 March 2011 event

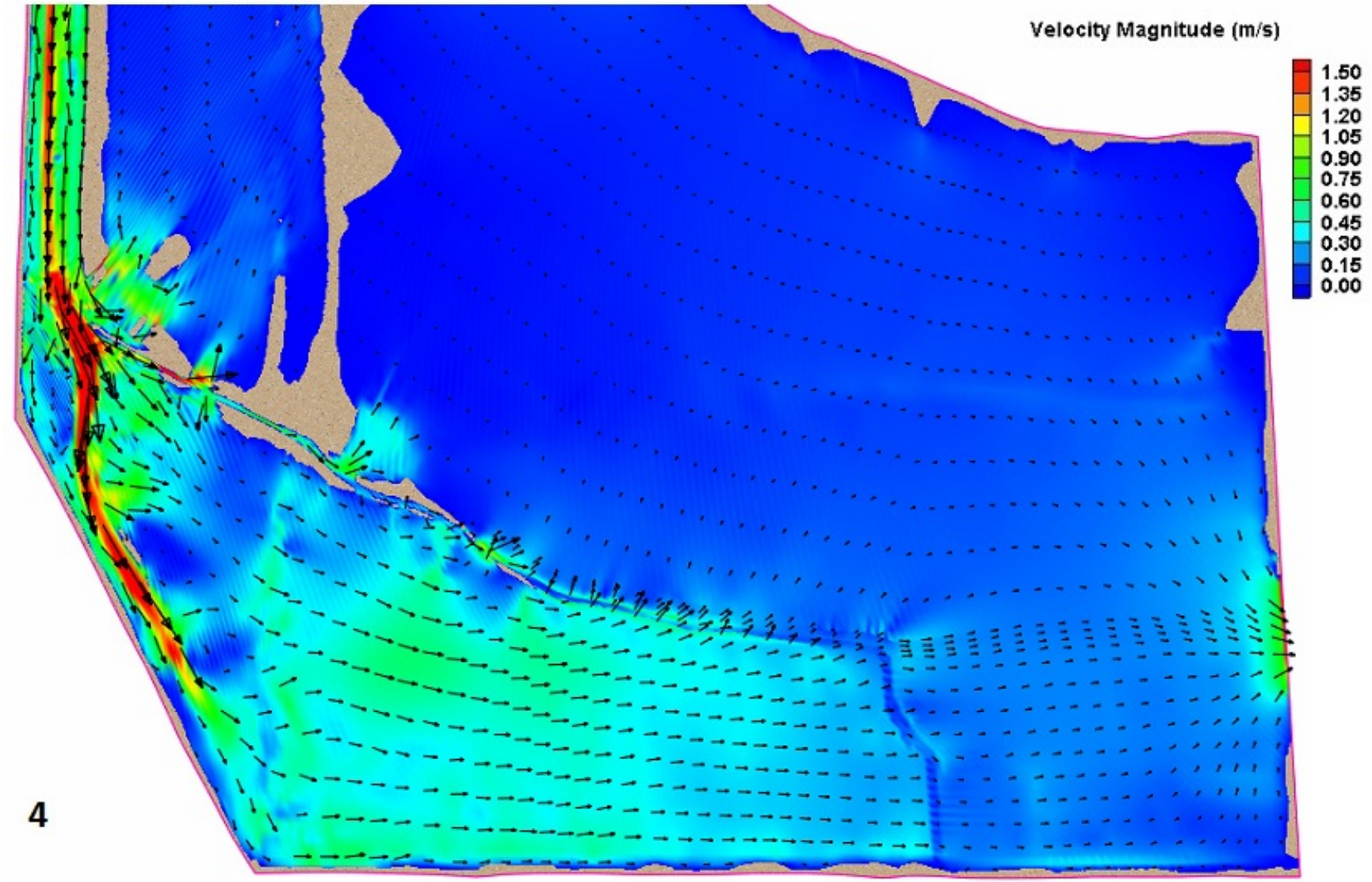


Figure 4.38 CCSB validation velocity magnitude result with scaled directional vectors, at selected time 4 of 23-27 March 2011 event

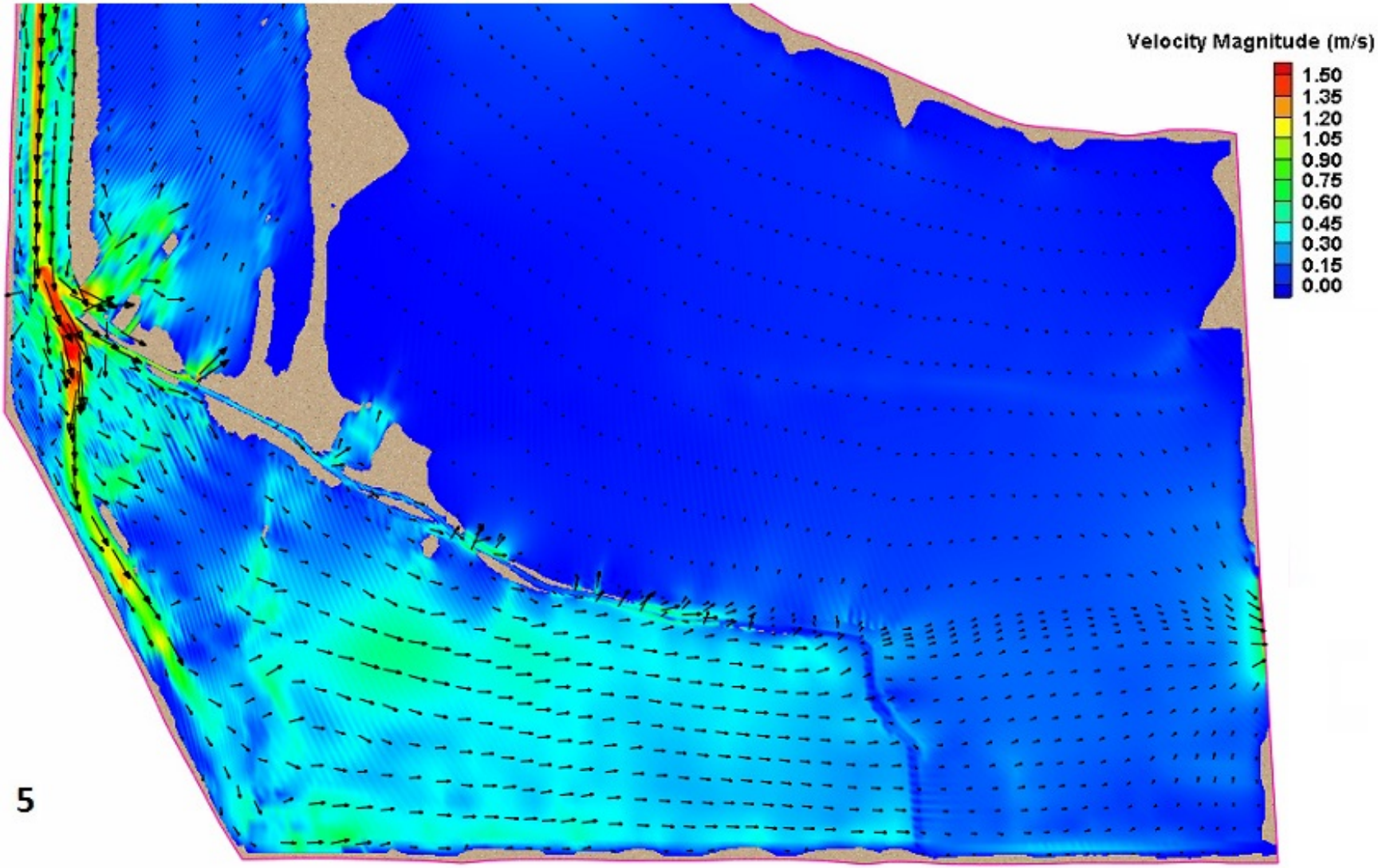


Figure 4.39 CCSB validation velocity magnitude result with scaled directional vectors, at selected time 5 of 23-27 March 2011 event

## 5 REFERENCES


Brazelton, W. (2010). "Rating Curve for Cache Creek Settling Basin Weir" EMAIL to Kara Carr. April 21, 2010.

De Vriend, D.J., (1999) Flow measurements in a Curved Rectangular Channel, Laboratory of Fluid Mechanics, Department of Civil Engineering, Delft University of Technology, Internal report no. 9-79.

Engelund, F. and Hansen, E. (1967). “A monograph on Sediment Transport in Alluvial Streams”. Teknish Vorlag, Copenhagen, Denmark.

Garbrecht, J., Kuhnle, R. and Alonson, C. (1995). “A Sediment Transport Capacity Formulation for Application to Large Channel Networks”. Journal of Soil and Water Conservation 50(5), 527–529.

Huang, Sui Liang (2007): "Effects of using different sediment transport formulae and methods of computing Manning's roughness coefficient on numerical modeling of sediment transport." Journal of Hydraulic Research, 45:3, 347-356

Jia, Y., and Sam S.Y. Wang, 2001a. *CCHE2D: Two-dimensional Hydrodynamic and Sediment Transport Model for Unsteady Open Channel Flows Over Loose Bed*. Technical Rep. No. NCCHETR- 2001-1, National Center for Computational Hydroscience and Engineering, The University of Mississippi. <http://www.ncche.olemiss.edu/sites/default/files/files/docs/cche2d/techmanual.pdf>

Jia, Y., and Sam S.Y. Wang, 2001b. *CCHE2DVerification and Validation Tests Documentation* Technical Rep. No. NCCHETR- 2001-2, National Center for Computational Hydroscience and Engineering, The University of Mississippi. <http://www.ncche.olemiss.edu/sites/default/files/files/docs/cche2d/validation.pdf>

Kantoush, S.A., De Cesare, G., Boillat, J.-L., Schleiss, A.J., 2008. "Flow field investigation in a rectangular shallow reservoir using UVP, LSPIV and numerical modeling." Journal of Flow Measurement and Instrumentation 19 (3-4), 139-144.

Mohanty, K. P., Dash, S. S., and Khatua, K. K. (2012). “Flow investigations in a wide meandering compound channel.” International Journal of Hydraulic Engineering, 1(6), 83-94.

Negm, A. M., Abdulaziz, T., Nassar, M., & Fathy, I. (2010). "Predication of life time span of High Aswan Dam Reservoir using CCHE2D simulation

model." In Proceeding 14th International Water Technology Conference (pp. 611-626).

Newton, C.T., 1951, “An experimental investigation of bed degradation in an open channel”, Transactions of the Boston Society of Civil Engineers, (pp. 28-60).

Proffit, G.T. and A.J. Sutherland, (1983). “Transport of Non-uniform Sediment”. Journal of Hydraulic Research 21(1), 33–43.

Rajaratnam, N. and Ahmadai, R. 1981, “Hydraulics of channels with flood-plains”, Journal of Hydraulic Research, IAHR, Vol. 19, No. 1, (pp. 43-60).

Rijn, L. C. van (1986). Manual sediment transport measurements. Delft, The Netherlands: Delft Hydraulics Laboratory

Soni, J. P. (1981). Laboratory study of aggradation in alluvial channels. *Journal of Hydrology*, *49*(1), 87-106.

Thayer, R. (2009) “Cache Creek Nature Preserve.” Putah and Cache: A Thinking Mammals Guide to the Watershed. University of California, Davis. June 8, 2009. <http://bioregion.ucdavis.edu/book/13_Lower_Cache_Creek/13_03_circ_ccnp.html>

Wang Sam S.Y., and Hu, K.K., 1992 “Improved methodology for formulating finite-element hydrodynamic models”, In T,J, Chung, (ed) Finite Element in Fluids, Volume 8, Hemisphere Publication Cooperation, pp 457-478.

Wu Weiming, and Sam S.Y. Wang (1999). “Movable Bed Roughness in Alluvial Rivers.” Journal of Hydraulic Engineering, ASCE, Vol. 125, No.12, pp.1309-1312.

Wu, Weiming, Sam S.Y. Wang, Y. F. Jia, (2000). “Non-Uniform Sediment Transport in Alluvial Rivers”. Journal of Hydraulic Research, 38(6).

## APPENDIX

Figure A.0.1 Dr. Ercan and Dr. Carr on the Sacramento River, ADCP Trial Run December 13, 2013

Figure A.0.2 Tracker Guide V-14 Boat purchased for sediment and velocity measurements within the CCSB

Figure A.0.3 ADCP transmitter and float